Report no. changed (Mar 2006): SM-360-UU

SACLANTCEN MEMORANDUM
serial no.: SM-360

SACLANT UNDERSEA RESEARCH CENTRE MEMORANDUM

LONG RANGE, LARGE THROUGHPUT RADIO DATA LINK FOR DUSS (DEPLOYABLE UNDERWATER SURVEILLANCE SYSTEMS)

L. Mozzone, A. Berni, P. Guerrini

October 1999

Report no. changed (Mar 2006): SM-360-UU

SACLANT Undersea Research Centre
Viale San Bartolomeo 400
19138 San Bartolomeo (SP), Italy

tel: +39-0187-5271
fax: +39-0187-527.420

e-mail: library@saclantc.nato.int

NORTH ATLANTIC TREATY ORGANIZATION

SACLANTCEN SM-360

Long range, large throughput radio data link for DUSS (Deployable Underwater Surveillance Systems)

Mozzone L., Berni A., Guerrini P.

The content of this document pertains to work performed under Project 021-1 of the SACLANTCEN Program of Work. The document has been approved for release by The Director, SACLANTCEN.

Jan L. Spoelstra
Director

intentionally blank page

Long range, large throughput radio data link for DUSS (Deployable Underwater Surveillance Systems)

Mozzone L, Berni A, Guerrini P

Executive Summary:

In the current security environment, the submarine threat is posed by small submarines operating in shallow coastal waters. These operating areas are characterized by heavy shipping traffic and strong reverberation conditions. These conditions lead to poor performance from currently operational sonar systems.

The DUSS (Deployable Underwater Surveillance Systems) concept is based on a network of autonomous sonar sources and receivers designed and deployed for optimal detection of small targets in adverse environmental conditions. Such distributed sensors rely on data communication to implement coordinated surveillance of the desired areas.

Experiments were carried out on radio transmission of large data flows across large distances from a deployed buoy to NRV *Alliance*.

This study reports the data collected and analyzes the results in terms of the features and constraints of the experimental and operational DUSS radio links.

Two mono-directional telemetry systems operating at frequencies of 0.4 and 2.28 GHz were tested with a 2 Mbps data throughput. The radio link was set up, antenna types and elevations were tested and configuration parameters were adjusted and optimized. The desired range of 10 n.mi was achieved. Field tests were supported by computer simulations to achieve better insight into link-balance equations, taking into account engineering and environmental parameters. The simulations validated the experimental results. An additional test assessed the performance of a full duplex spread-spectrum data link operating at 2.4 GHz with a data rate of 128 kbps up to 3.5 n.mi. which is being subjected to further study.

The experiments conclusions provide useful inputs to the design of a functional DUSS system. Further development and analysis is recommended on the topics of radio propagation, modulation and coding schemes.

intentionally blank page

SACLANTCEN SM-360

Long range, large throughput radio data link for DUSS (Deployable Underwater Surveillance Systems)

Mozzone L, Berni A, Guerrini P

Abstract:

Two mono-directional radio telemetry systems are described operating from a buoy to NRV *Alliance* at frequencies of 0.4 and 2.28 GHz. Digital data at 2 Mbps were transmitted close to the sea surface, collecting information on error statistics and propagation loss *versus* buoy distance, antenna height and radio parameters. A candidate system was configured for both frequency bands and the goal of 10 n.mi range was achieved. Field tests were supported by computer simulation for validation and a better insight into the results. An additional test assessed the performance of a low-power, full duplex, spread-spectrum radio link, operating at the data rate of 128 kbps, up to 3.5 n.mi. The experiments and conclusions provide useful input to the design of a Deployable Underwater Surveillance System (DUSS) for scientific and operational purposes.

Keywords: Buoy-to-buoy communication – Deployable Underwater Surveillance System – computer networks – data communication – distributed systems – radio propagation – spread spectrum communications – wireless communications

Contents

1

Introduction

This report describes a key phase in the study and development of a demonstrator and experimental test system for deployable underwater surveillance systems (DUSS) [1,2,3,4,5]. DUSS require the transmission of large data volume (around 2 Megabits per second per link) to a centralized acquisition and processing system from autonomous units deployed up to 10 n.mi away. The design of this multistatic network of autonomous active sonar receivers includes therefore long-range wireless communication links. A radio link was chosen for flexibility and lower cost compared to fiber optics or electric cable. The prototype receiver for DUSS will be used with the new radio link as a tool for future tests at sea, together with other 4 multistatic units, planned for the next years. Those units will enable the testing at sea of wide multistatic deployment patterns.

The "DUSS 98" experiments were conducted in November 1998 to collect data on the critical subject of radio propagation close to the sea surface, in terms of error statistics and propagation loss.

Two channels (0.4 and 2.28 GHz) were tested with different antenna heights (on the sonobuoy side). The first part of the experiment was performed with ITS *Ponza* simulating the deployed sonar receiver, to simplify modifications to radio and antenna parameters. Once a satisfactory setting was achieved, final proof of the system performance was obtained transmitting from a buoy (fixed antenna height). ITS *Ponza* monitored the buoy and provided radar localization and assistance. NRV *Alliance* carried the receiving radio station. The new digital telemetry system and code were tested, in conjunction with the prototype radio units.

An additional experiment assessed the performance of a different link (full duplex data connection through spread spectrum radio). The adoption of fully featured digital wireless networks appropriate to the distributed structure of the DUSS concept.

2

Background and technical objectives

The radio links so far tested with DUSS provide either 0.24 Mbps at 250 MHz with a maximum operational range of 5 n.mi, or 6.1 Mbps at 2.28 GHz with a 7 n.mi maximum range. These ranges are referred to a bit error rate (BER) around $3\,10^{-3}$ and 10^{-6} respectively. The former rate turned out to be an acceptable lower boundary for sonar research applications. Corrupted samples are usually isolated and can be discarded without compromising effective echo analysis. The latter error rate is closer to commonly adopted specifications for radio links.

The 2.28 GHz link is more than one order of magnitude more expensive than the 250 MHz link, but it is capable of delivering larger data throughputs, which are required by some applications such as sonar operation.

While the 250 MHz system is capable of reaching a range of 5 n.mi with a small surface unit, the existing 2.28 GHz radio buoy has a 6 m mast, which constitutes a limiting factor for buoy size, geometry and handling. The 250 MHz link was replaced by a new link operating in the 400 MHz frequency range, in order to accommodate larger bandwidth requirements and to obtain more favourable radio coverage properties.

Our research concentrates on the study of critical engineering parameters Transmitter power seems to be less critical than antenna height and channel frequency. High-gain directional antennae on the receiver side contribute to reducing the effect of noise and interference, but pose constraints to ship maneuverability and buoy deployment geometries.

The present work defines the system configurations required to extend performance to 10 n.mi ranges. It also provides a useful experimental analysis of parameter-performance tradeoffs.

3

Assets, systems and operations

The following sections describe the assets that were used in the experiments, the test area and the operations (see also Annex A).

3.1 ITS Ponza

This vessel, offered by the Italian Navy, simulated the deployable sonar unit, transmitting a simulated data flow using a radio transmitter and antenna mast. Antenna height and radio parameters could therefore be adjusted during the tests. ITS *Ponza* also monitored the DUSS buoy.

3.1.1 Assets onboard ITS Ponza

- Signal generators and encoders, simulating a data flow of 2 Mbps, of which 2 Mbps of useful payload.
- 2.28 GHz radio transmitter, 6 W transmit power.
- DUSS prototype transmitting telemetry chain.
- 2.28 GHz antenna, 8.7 m above sea level, vertical polarization.
- 400 MHz radio, 4.5 / 20 W transmit power.
- 400 MHz antenna, positioned 7.8 or 13.7 m above sea level, vertical polarization.

3.2 Assets onboard Radio buoy

- 400 MHz radio, 20 W transmit power.
- Omnidirectional transmitting antenna positioned 6 m above sea level, vertical polarization.

3.3 NRV Alliance

NRV *Alliance* hosted the receiving data station, emulating the operational DUSS functions.

3.3.1 Assets onboard NRV Alliance

- 2.28 GHz and 400 MHz receivers.
- DUSS prototype receiving telemetry chain.
- 2.28 GHz directional antenna (22 dB gain) positioned at 33 m above sea level, vertical polarization.
- 2.28 GHz directional antenna (17 dB gain) positioned at 26 m above sea level, vertical polarization.
- 400 MHz omnidirectional antenna positioned at 5 and 33 m above sea level, vertical polarization.
- 400 MHz directional antenna (Log-periodical 5 dB gain) positioned at 26 m above sea level, vertical polarization.
- 400 MHz directional antenna (Yagi, 10 dB gain) positioned at 26 m above sea level.
- Pre-amplifiers, low loss cables.
- Radio receivers with computer log of signal level and error count at 5 s intervals.
- Computer log of transmitter – receiver range.
- AREPS: Advanced Refractive Effects Prediction System (RF propagation model distributed by SPAWARSYSCEN, San Diego).
- MATLAB: simple reflection of signal over flat sea surface, no phase reversals.

3.4 Test area

Several runs were performed in the 15 n.mi × 6 n.mi area defined in the test plan, 10 n.mi off Viareggio - Livorno). The two units, ITS *Ponza* (transmitter) and NRV *Alliance* (receiver) moved alternately in order to optimize efficiency (time) and data quality (antenna orientation). 15 straight runs were performed at a typical speed of 6 kn, for up to 2 h, representing the best trade-off between test duration and the number of samples collected. Stations at maximum radio ranges were kept to collect additional statistics for the various data link configurations.

A 400 MHz buoy was deployed on 18 and 19 November 1998, reproducing the real case. ITS *Ponza* assisted the buoy, showed its position and transmitted reference signals for comparison. Various antennae, cabling, amplification settings were tested for the new 400 MHz link, finally yielding (on 19 November) an optimal configuration, which fulfilled the objective of 10 n.mi ranges.

4

Experimental data

The following measurements were taken: sea surface conditions, atmospheric visibility, received signal level, noise level, bit error count averaged at 5 s intervals, bit error probability computed at 30 s intervals. Signal quality was monitored with spectrum analyzers and oscilloscopes, in an attempt to discriminate plain signal attenuation effects from symbol distortion due to multipath. For this purpose, a reference sinusoidal signal was encoded in the data, for immediate evaluation. Range information was extracted from radar tracks recorded by NRV *Alliance*.

Experiments were performed in sea states between 3 and 4 (with occasional whitecaps) and winds ranging from 5 to 20 kn. Visibility was very good on November 17 and 19, 1998, good but cloudy on November 18)

4.1 Results

The following figures show some of the data collected. Further analyses are presented in Sect. 5.

For each test case, three plots are presented, showing signal level at the receiver input, in dBm[1] (see Sect. 5.2.1), bit error rate (BER) after decoding and parity check, averaged over a 5 s period or 16 min at 2.28 GHz, 3 min at 400 MHz.

The averaging windows are small enough to collect statistically valid data representing homogeneous, quasi-stationary conditions. The 2 Mbps data rate leads to the collection of 10^6 samples in 5 s, $1.9 \cdot 10^9$ samples in 16 min.

All measurements are plotted *versus* transmitter-receiver range in n.mi.

[1] In the previous sections and later in the text, we represent power measurements using the dBm unit. Decibels always represent power ratios: in order to express a power P in dB, we divided *P* by one milliwatt, as follows:

$$P_{dBm} = 10 \log_{10} \frac{P}{1mW}$$

dBm (decibel-milliwatts), is commonly used in communications engineering, in consideration of the small powers that are usually involved.

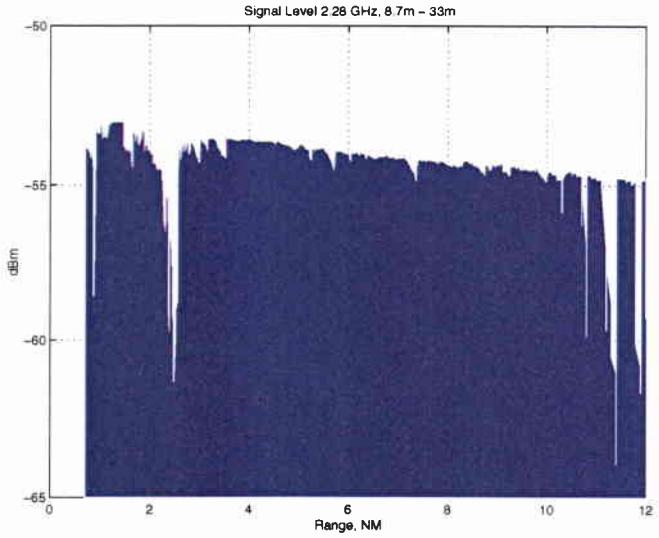

Figure 1 *Signal level versus range, 2.28 GHz-6W, 8.7 m transmitter antenna, 33 m directional receiver antenna. Calibrated level in dBm. From comparisons with BER data (below) it is however evident that the threshold of good transmission is around 55 dBm.*

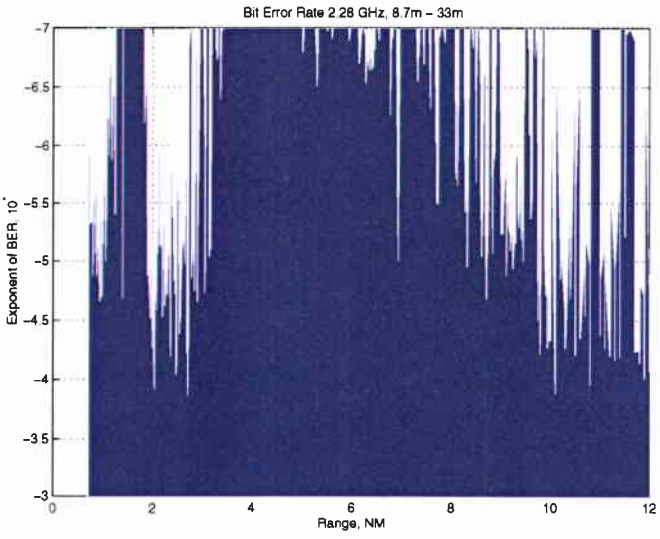

Figure 2 *Bit Error Rate (BER) versus Range, 2.28 GHz-6W, 8.7 m transmitter antenna, 33 m directional receiver antenna. Errors occur in bursts.*

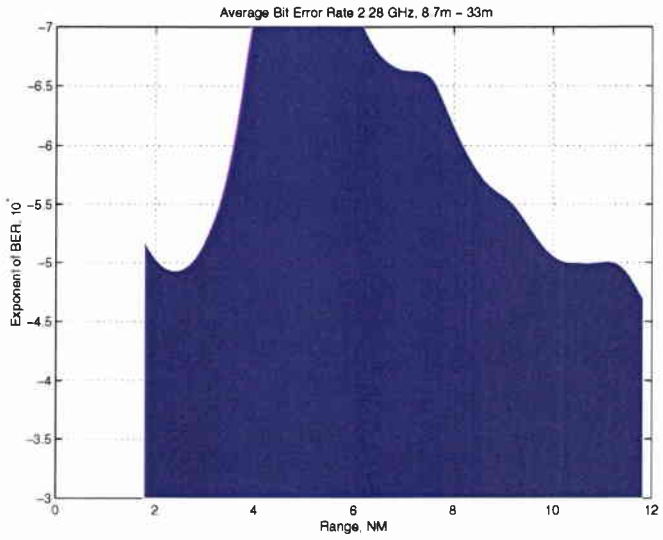

Figure 3 *Bit Error Rate (BER) versus Range, 2.28 GHz-6W, 8.7 m transmitter antenna, 33 m directional receiver antenna. The raw data of Fig. 2 are averaged here with a sliding window of 16 min. These data are representative of average channel availability (error bursts just interrupt the link).*

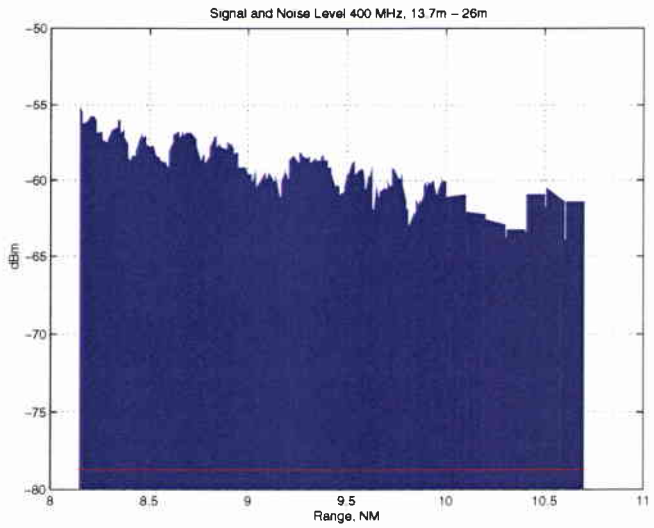

Figure 4 *Signal level versus range, 400 MHz-20W, 13.7 m transmitter antenna (Ponza), 26 m directional receiver antenna. Calibrated level in dBm with average noise level (red line).*

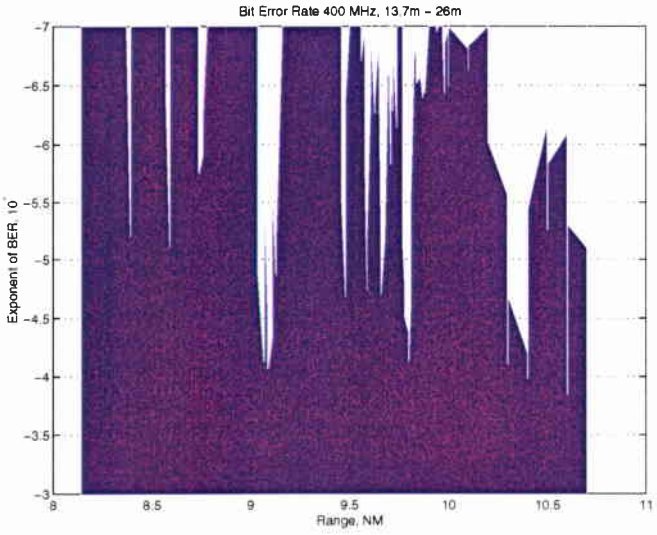

Figure 5 *BER versus range, 400 MHz-20W, 13.7 m transmitter antenna (Ponza), 26 m directional receiver antenna.*

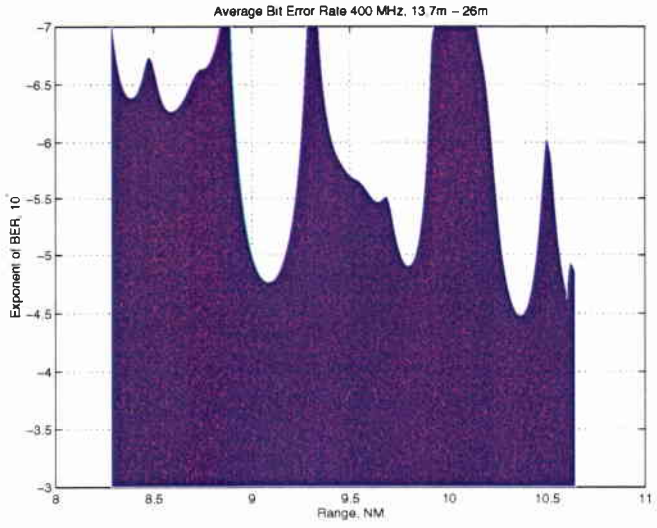

Figure 6 *BER versus range, averaged with sliding window, 400 MHz-20W, 13.7 m transmitter antenna (Ponza), 26 m directional receiver antenna.*

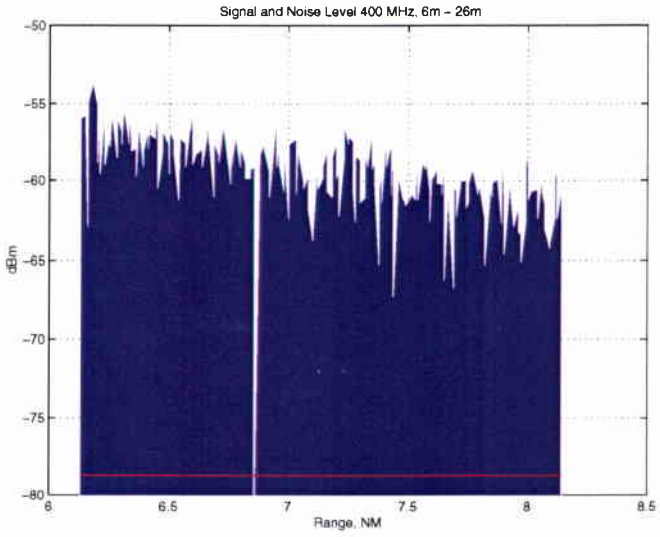

Figure 7 *Signal level versus range, 400 MHz-20W, 6 m transmitter antenna (Buoy), 26 m directional receiver antenna.*

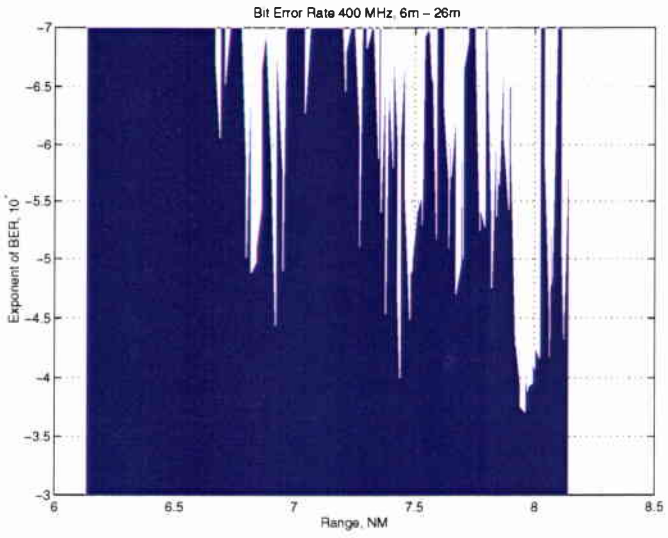

Figure 8 *BER versus range, 400 MHz-20W, 6 m transmitter antenna (Buoy), 26 m directional receiver antenna.*

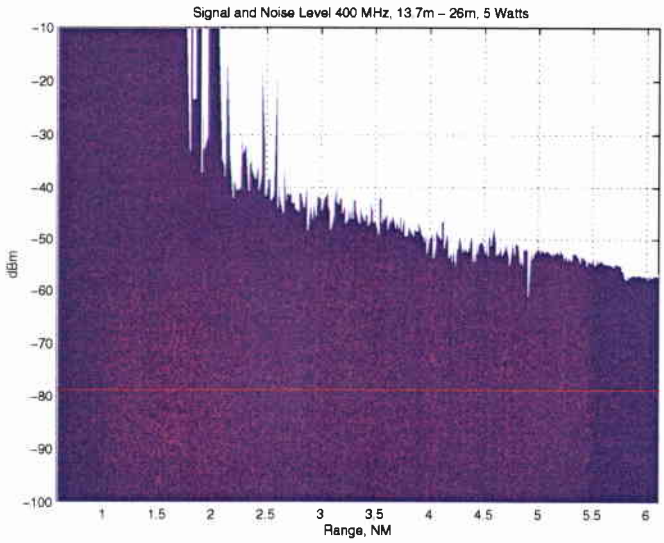

Figure 9 *Signal level versus range, 400 MHz, 13.7 m transmitter antenna at 5 Watts (Ponza), 26 m directional receiver antenna.*

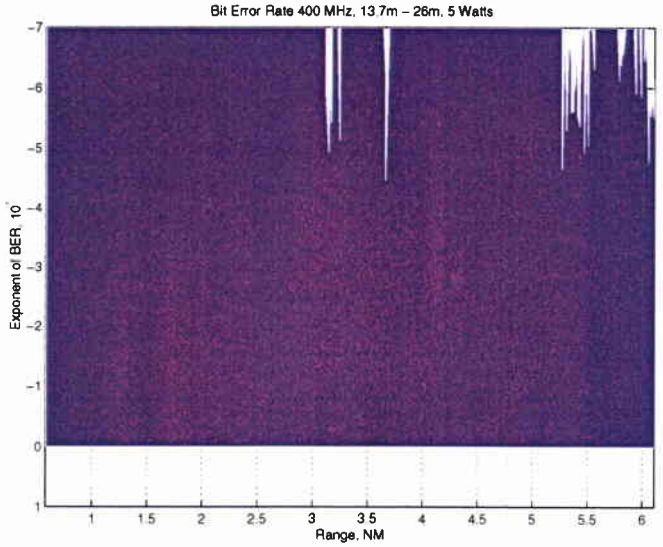

Figure 10 *BER versus range, 400 MHz, 13.7 m transmitter antenna at 5 Watts (Ponza), 26 m directional receiver antenna.*

Signal level plots show the general slope of propagation loss with increasing range. Signal slopes range from -45 to -55 dBm (2.28 GHz) and from -55 to -63 dBm (400 MHz) between 8 n.mi and 10 n.mi distances.

A macroscopic loss of signal has been measured around 2.5 n.mi, at 2.28 GHz. As shown in the following analysis, this is due to multipath, i.e. destructive interaction with the sea surface. Loss of signal occurs at shorter distances for lower transmitting antenna, i.e. 1.2 n.mi using a 6 m antenna mast. This abrupt signal loss has not been observed in the 400 MHz link, where antenna height and channel wavelength create a less critical configuration.

Signal fluctuations are also evident. They cannot be accurately predicted, but strongly influence error statistics and link quality, hence the importance of field tests. The extent of fluctuations at 2.28 GHz clearly increases with range, finally reaching the link outage threshold, with variations in excess of 7 dB. This is not the case for the 400 MHz link, where signal fading and link loss occur in a progressive manner, with fluctuations limited to 2-3 dB.

The BER data show either errors averaged in 5 s intervals or in longer windows (16 min for 2.28 GHz, 3 min for 400 MHz data). In the first case (Figs. 2, 5, 8, 10), the error bursts are evident, corresponding to the signal fading discussed above. Error bursts were observed at very brief intervals (less than one second). This fact suggests a channel model where complete loss of the data link alternates with intervals of excellent transmission, especially in the 2.28 GHz case where signal levels fluctuated and BER plots show isolated spikes. When approaching the maximum operating distance, the 400 MHz link is subject to a more continuous and regular signal fading associated with error bursts, with shorter intervals of reliable data transmission.

The smoothed curves (Figs. 3 and 6) show link performance in terms of the overall expected rate of availability of the channel. For example, 10^{-5} means either that 99.999% of data are correctly delivered, or that the link is capable of delivering its nominal throughput for 99.999% of the time. This type of measurement can be achieved through a proper error-detection coding.

A fully operational data acquisition system is being set up, where digital samples are stored on a computer file to permit more accurate measurement of error statistics. In particular, information on the duration of error bursts and maximum instantaneous BER can lead to the development of specifically optimized data formats and protocols. The experience with existing radio frequency (RF) equipment indicates transmission of very small data blocks (e.g. 1 single acoustic sample from all hydrophones) with a simple error detection code. In fact, the loss of sparse samples does not affect the quality of acoustic measurements, up to a maximum BER around 10^{-3}.

Figures 7 and 8 show measurements for the 400 MHz-20W link when the transmitting antenna is lowered to 6 m above sea level, as in the present DUSS buoy. A lower antenna results in a smaller transmission range. In this setup, signal levels between -54 and -65 dBm are measured at shorter ranges (6-8 n.mi). Signal fluctuations are more pronounced, with frequent error bursts of short duration.

Figures 9 and 10 show measurements at 400 MHz, transmitting from the tall antenna mast (13.7 m), this time with reduced power (5 W). Beyond 6 n.mi link performance drops dramatically. Up to that range, signal fluctuations decrease with range and are

limited. Signal level (-60 dBm) is 5 dB lower that the 20 W, 6 m case. This shows that higher antenna masts have a positive effect in reducing fluctuations: it also suggests that a low transmitter antenna cannot be compensated by higher transmitter power.

4.2 Spread-spectrum link

Similar measurements were collected with a low power, spread-spectrum link working at the data rate of 128 kbps, (Annex D). These results are not comparable to the above data, but represent an initial experimental assessment of the performance of this developing family of communication resources in the distinctive environmental conditions of sonar research. Satisfactory error rates (considerably better than 10^{-3}) were obtained, with temporary interruptions, up to 3.5 n.mi and beyond.

4.3 On-field simulations

The AREPS model [6] was used to reconstruct the results during the execution of the tests. The following plots show the limits of good data transmission *versus* antenna height and range for the two tested radio links (Figs. 11 and 13). The model can be used to extrapolate experimental data and predict SNR increase (in dB) that could be obtained with greater antenna heights (Figs. 12 and 14).

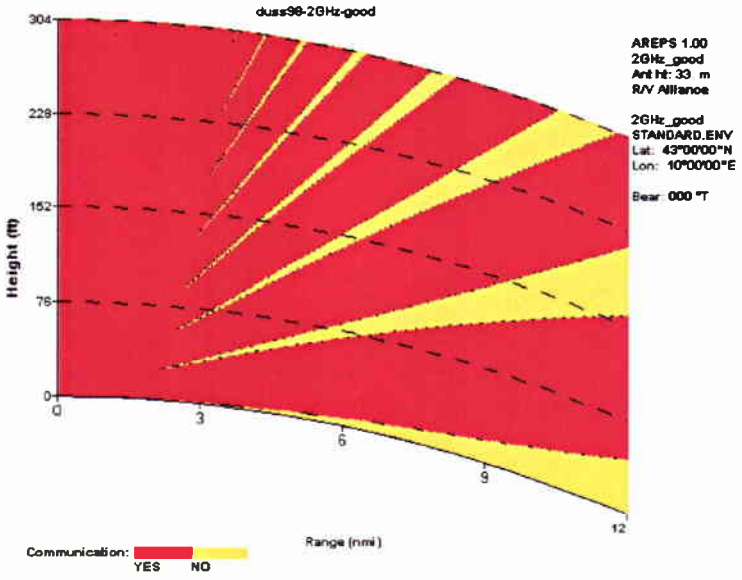

Figure 11 *AREPS output for 2.28 GHz link.*

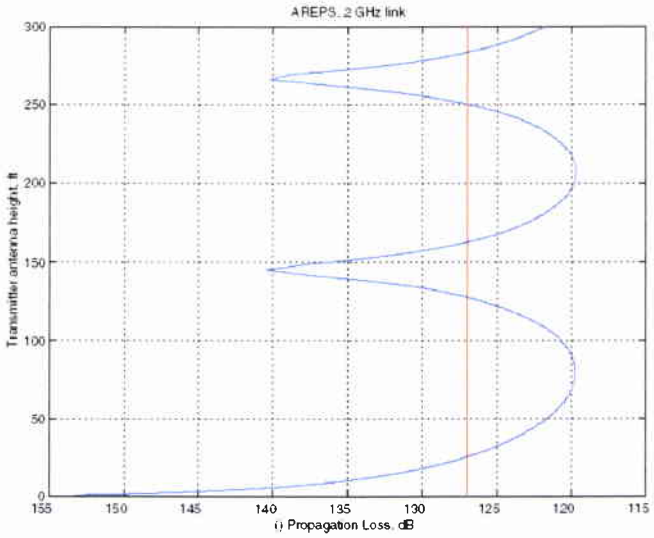

Figure 12 *AREPS output for 2.28 GHz link. Propagation Loss versus transmitter antenna height at 10 n.mi.*

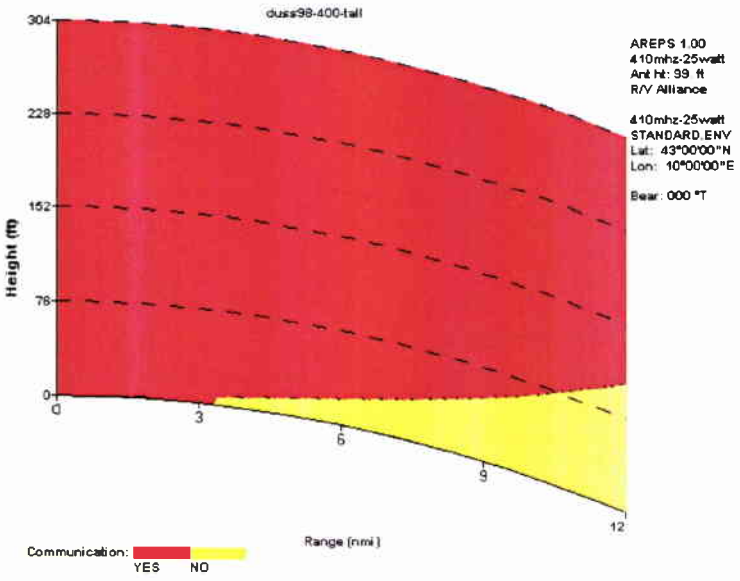

Figure 13 *AREPS output for 400 MHz link.*

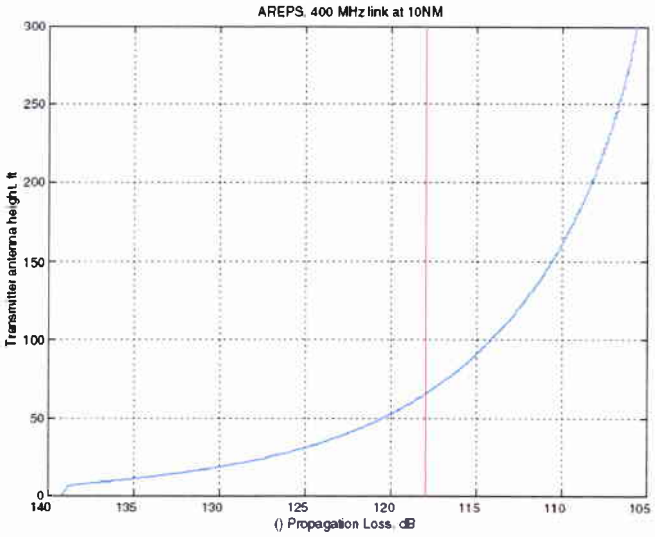

Figure 14 *AREPS output for 400 MHz link. Propagation Loss versus transmitter antenna height at 10 n.mi.*

Note that AREPS includes the receiver-gain term (composed of antenna gain, pre-amplifier gain, noise figure) in the propagation loss thresholds (shown as the red-yellow edge in Figs. 11 and 13 and as a red line in Figs. 12 and 14). These thresholds are therefore different for the two systems tested.

It must also be noted that the 400 MHz link is affected by a lower transmission loss. It also presents more regular patterns but requires taller antennae on the buoy side.

4.4 Summary of measurement results

- The existing 2.28 GHz radio link achieves the objective of 2 Mbps at 10 n.mi with a good BER (average 10^{-5} with periods at 10^{-4}). Antenna mast is 8.7 m, transmitter power is 6 W.

- A new link was set up at 400 MHz, with the data rate of 2 Mbps. It reaches 10 n.mi with an average BER between 10^{-5} and 10^{-7} and a peak BER of 10^{-4}. Its performance stability is more pronounced, but it requires a 13.7 m mast, given the longer wavelength and 20 W transmitter power.

- The 400 MHz link is capable of delivering the required quality up to the range of 6 n.mi retaining the 13.7 m mast, while reducing transmission power to 5 W. Using a 6 m short mast and 20 W transmit power, range is limited to 7 n.mi. In the latter setup, link quality is adversely affected by stronger fluctuations.

- All configurations require a directional receiving antenna.
- Antenna height on the buoy is the most critical parameter. The high mast required by the 400 MHz system is not well suited to a deployable system such as DUSS.
- The 400 MHz link requires more transmission power, however radio equipment is less expensive.
- The 400 MHz is expected to be less sensitive to weather conditions.
- For both the links examined, experimental results match with models, which are used in the following section for analysis.

5

Link-balance analysis and propagation simulations

This section introduces the theory of radio propagation close to the sea surface. It then presents the "link-balance equation", the equivalent of the sonar equation for radio links. By means of a propagation model, it finally reconstructs the link-balance equation terms for the configurations tested, thus providing an effective tool to validate and understand the experimental results reported.

5.1 Line-of-Sight range

RF propagation at frequencies above 2 GHz occurs *essentially* (but not exclusively) in line-of-sight (LOS) conditions. Lower frequencies (such as 400 MHz) are not limited to LOS, but can be included in our discussion, as the RF links tested were always within LOS range. Figure 15 shows the minimum height over the horizon of the radio link between two antennae 10 n.mi apart. The first is 6 m high (deployed buoy). The second has a variable height, shown on the horizontal axis and represents the receiver unit, either on another deployed buoy or on a ship. Antennae on the mast of NRV *Alliance* range from 26 to 33 m. The radio path is always well above the sea surface. The same does not hold for buoy-to-buoy links, which require very tall buoys or shorter ranges.

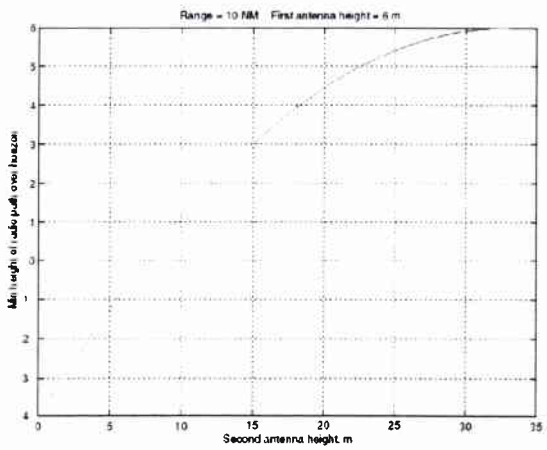

Figure 15 *Minimum path height over the horizon versus transmitter antenna height. Receiver antenna: 6 m above sea level*

The maximum achievable range of LOS propagation, limited by the earth curvature, can also be expressed by the following formula:

$$range \cong 1.065(\sqrt{h_t} + \sqrt{h_r}) \qquad (5.1.1)$$

where h_t is the transmitter height and h_r is the receiver height, expressed in feet. If transmitter and receiver heights are expressed in meters, Eq. (5.1.1) is modified as follows:

$$range \cong 1.929(\sqrt{h_t} + \sqrt{h_r}) \qquad (5.1.2)$$

The resulting range is expressed in n.mi in both cases. Table 1 shows some results relating to experiment configuration. Buoy to buoy links are critical, unless tall masts are used.

	Transmitter antenna height	*Receiver antenna height*	*Maximum theoretical range*
Short buoy – ship	6 m	33 m	15.8 n.mi
Medium buoy – ship	8 m	33 m	16.5 n.mi
Tall buoy - ship	14 m	33 m	18.3 n.mi
Buoy – buoy	6 m	6 m	9.5 n.mi
Tall buoy – tall buoy	14 m	14 m	14.4 n.mi

Table 1 *Formula (5.1.2) applied to some of the experimental configurations.*

5.2 Link-balance equation: free space propagation loss

As demonstrated by the experiments, LOS conditions do not guarantee successful data transmission. The *actual* range that is achieved by a communication system can be calculated by the means of a *link-balance equation*, where signal quality at receiver input is estimated and compared with receiver sensitivity, taking into account the characteristics of both the system and the environment.

The simplest case of electromagnetic wave propagation is *free space propagation*, that is, propagation in a region of space the properties of which are isotropic and homogeneous. In this section we demonstrate the relationship between transmission power, antenna characteristics and radio frequency. We start by presenting the isotropic radiator, an ideal

omnidirectional antenna. We will then consider antenna gain and directivity issues related to power received at the receiver. Antenna gain will be used as one of the variables of link-balance equations.

Electromagnetic waves propagate from a transmitting antenna: the antenna acts as a transducer converting electric signals into electromagnetic fields. The receiver antenna performs the reverse function, converting electromagnetic fields into electric signals.

Assuming that the antenna radiates a power P_T (expressed in W) in an omnidirectional way, that is, it transmits uniformly over 4π steradians. Such a source is an *isotropic radiator*. The *radiated power flux density*, ρ, measured on a spherical surface at the distance of r m from the source, is related to transmitted power by

$$\rho = \frac{P_T}{4\pi r^2} \ [\mathrm{W/m^2}] \tag{5.2.1}$$

as $4\pi r^2$ is the area of the sphere. The power, P_R, extracted with the receiving antenna, can be expressed as

$$P_R = \rho A = \frac{P_T A}{4\pi r^2} \ [\mathrm{W}] \tag{5.2.2}$$

where A is the absorption cross section (*effective area* or *equivalent aperture*) of the receiving antenna, defined as

$$A = \frac{total\_power\_extracted}{incident\_power\_flux\_density} \tag{5.2.3}$$

A is expressed in $\mathrm{m^2}$.

Transmitting antennae concentrate the radiated power in one lobe are called *directive antennae*.

Their directivity is quantified by *antenna directivity, D*, that relates the antenna power output to that of an isotropic radiator, using exclusively geometric criteria.

$$D = \frac{Power\_flux\_density\_at\_range\_r\_in\_direction\_of\_\max\_radiation}{Mean\_power\_flux\_density\_at\_range\_r} \tag{5.2.4}$$

If no dissipation occurs, *antenna gain*, G, in the direction of maximum intensity, equals antenna directivity D in Eq. (5.2.4). We can increase the flux radiated by the antenna, by leaving transmission power untouched and increasing antenna directivity and consequently its gain.

In a dual way, D and G can be defined also for receiving antennae, while the definition of A can be extended to transmitter antennae.

The relationship between antenna gain, G and the effective area, A, can be written [14] as

$$G = \frac{4\pi A}{\lambda^2} \tag{5.2.5}$$

where λ is the wavelength of the signal carrier (in meters). It shows that, as with acoustic arrays, gain increases with aperture and frequency. Wavelength and carrier frequency are related through the following equation

$$\lambda = \frac{c}{f} \tag{5.2.6}$$

where $c = 3 \cdot 10^8$ m/s is the speed of light constant.

The definition of G enables us to define the *effective radiated power* (EIRP) for an isotropic radiator. EIRP is the product of transmitted power P_t and transmitter antenna gain G_T. It permits computation of the real radiated power flux density in the main lobe of the directive antenna.

$$EIRP = P_T \cdot G_T \tag{5.2.7}$$

EIRP is not only an important radio engineering parameter, but also a measure which is used to determine the compliance of radio transmission equipment to licensing requirements, which usually impose limits on radiated flux power density, in order to reduce risks of interference. Considering EIRP, Eq. (5.2.2) can now be re-written as follows:

$$P_R = \rho A = \frac{EIRP \cdot A}{4\pi r^2} \tag{5.2.8}$$

The effective area of the receiver antenna can be calculated from Eq. (5.2.5), solving for A as follows:

$$A = \frac{\lambda^2}{4\pi} \cdot G_R . \tag{5.2.9}$$

To find the received power P_R we will substitute Eq. (5.2.9) into Eq. (5.2.8) to obtain

$$P_R = \frac{P_T \cdot G_T \cdot G_R}{(4\pi r / \lambda)^2} = \frac{P_T \cdot G_T \cdot G_R}{L_{FS}} \tag{5.2.10}$$

where L_{FS} is *free space propagation loss*.

For clarity, we can also explicitly express free space propagation loss as the ratio between transmitted power and received power with omnidirectional transmit and receive antennae. Assuming transmit and receive antennae with unit gain G_T and G_R defined as in Eq. (5.2.5), we can write the following expression:

$$L_{FS}[dB] = 10\log\frac{P_T}{P_R} = 10\log G_T - 10\log G_R + 10\log\left(\frac{\lambda}{4\pi r}\right)^2 =$$
$$= 10\log G_T + 10\log G_R + 20\log\left(\frac{c}{\frac{f_{Hz}}{4\pi r}}\right) \qquad (5.2.11)$$

Which can be rewritten as

$$L_{FS} = 10\log G_T + 10\log G_R - 20\log(f_{Hz}) - 20\log(r) + 147.56dB \qquad (5.2.12)$$

This leads to the fundamental expression of free-space propagation loss for unity-gain transmit and receive antennae and unobstructed line-of-sight transmission:

$$L_{FS} = -32.5 - 20\log(r) - 20\log(f_{MHz}) \qquad (5.2.13)$$

where r in the range in km between transmitting source and receiver and f_{MHz} is the signal's central frequency, in MHz. This is a typical expression which appears as the sum of two terms. The first accounts for spherical spreading of the signal wavefront with distance. The second measures the frequency-dependent signal attenuation. As frequency increases, A of the omnidirectional antenna decreases, thus intercepting a lower power. This affects the resulting signal–to–noise ratios at the receiver and the specifications of preamplifier noise when high frequencies are used.

It is also possible to express the frequency in GHz: in this case the formula is to be modified as in Eq. (5.2.14)

$$L_{FS} = -92.5 - 20\log(r) - 20\log(f_{GHz}) \qquad (5.2.14)$$

The 20log(f) term varies with frequency. Propagation loss at 10 n.mi at 2.28 GHz will be 15 dB higher than at 400 MHz, without considering other environmental effects. In Sect. 7 we will present an accurate comparison of propagation loss for the two frequencies, in free space and in a realistic environment.

We can observe from Eq. (5.2.5) that the gain of a fixed size antenna increases with decreased wavelength (increased frequency). It also increases with increased effective area. Increasing transmitter antenna gain is equivalent to concentrating radiated power in a more restricted cone angle, where the electromagnetic flux density will be proportionally higher. This means that a higher antenna gain will imply narrower beamwidths. In our experiments we tested omnidirectional antennae on the transmitter

side and directional antennae on the receiver side. A directional antenna on the receiver side permits exploitation of directivity gain to limit noise and interference effects.

5.3 Optical interference and surface reflections

In a realistic environment, propagation loss is affected by reflections from the earth surface, the atmosphere and man made objects, which cause *multipath scattering*. Multipath improves link quality as long as the phase of the reflected signal is similar to that of the primary (non-reflected) signal. If the phase shift approaches 180°, link quality will be adversely affected.

When an electromagnetic wave hits the ocean surface, a major fraction of the energy is reflected and continues to propagate along a reflected path. The strength of the reflected wave is determined by the reflection coefficient, a value which is a function of the frequency and polarization of the electromagnetic radiation, the grazing angle of the wave and the roughness of the sea surface.

For small grazing angles and calm seas, the reflection coefficient approaches unity, that is, the reflected ray is almost as strong as the direct one. As wind speed increases, the reflection coefficient will decrease, due to sea surface roughness.

Multipath scattering in a marine environment is strongly influenced by the sea state: calm seas will better reflect electromagnetic waves. As a consequence, multipath effects caused by interference of out-of-phase signals will be maximized. On the other hand, conditions of high winds will limit the sea reflectivity and the effects of multipath reception will be less relevant.

Reflected waves are subject to a phase rotation of roughly 180° for horizontally polarized signals.

When two or more wave trains meet, after travelling through different paths, multipath interference takes place. If the waves arrive in phase, interference has a *positive* effect, so that the strength of the resulting electric field is higher, compared to the primary wave. In the other case, multipath interference will have a *destructive* effect and the strength of the received signal will be substantially decreased.

Varying the positions of transmitter and receiver, the relative lengths of the direct and reflected paths will vary accordingly: the result will be that direct and reflected waves will be subject to a variable phase difference. The received signal, resulting from the vector sum of direct and reflected waves, may even be completely cancelled.

The magnitude and phase of the reflection coefficient for vertically polarized signals behave differently from waves with horizontal polarization, as illustrated in Figure 15a.

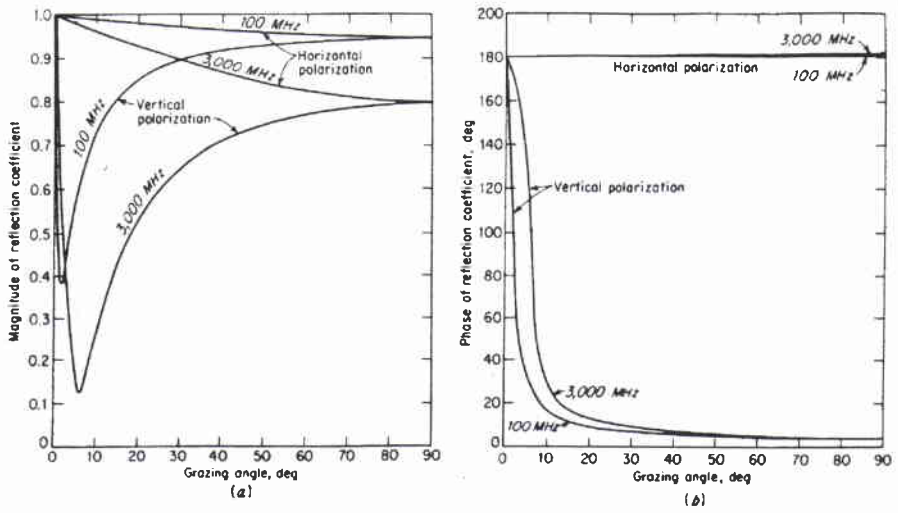

Figure 15A *Reflection coefficient magnitude and phase.*

The angle corresponding to minimum coefficient is named Brewster's angle (about 7° grazing angle at 3 GHz) [15].

Large length differences between direct and reflected path may lead to delay at the receiver, with a limiting impact on the usable bandwidth.

5.4 Effects of environmental parameters on RF propagation

The design of a wireless link requires careful consideration of the environmental parameters which characterize the area in which the link will be deployed. Atmospheric conditions noticeably affect radio propagation, though not in a measure comparable to the interactions between acoustic waves and sea water characteristics.

In commercial practice, systems are designed considering annual or worst-month climate factors, so that reliable service can be assured over a period spanning several years. Tactical links such as those supporting DUSS are deployed for limited periods of time, so their design may be optimized to accommodate the specific climate conditions for those periods.

5.4.1 Refraction index

The term *refraction* identifies the property of a transmission medium of bending electromagnetic waves when they travel through the medium. Refraction can be measured by a *refraction index*, n, defined as the ratio between the speed c of propagation in free space and the speed v of propagation in the medium. The normal value of n for the atmosphere layers close to the earth surface varies between 1.000250 e 1.000400.

For radio propagation studies, the index of refraction is not a convenient number, therefore a scaled refraction index, N, termed *refractivity* has been defined.

At microwave frequencies and below (including 400 MHz and 2.28 GHz), the relationship between the index of refraction n and N for air that contains water vapour is given in [7] as

$$N = (n-1)10^6 = 77.6\frac{p}{T} + 3.73 \cdot 10^5 \frac{e}{T^2} \qquad (5.4.1)$$

where e is the partial pressure due to water vapour (in millibar), obtained from the following equation:

$$e = \frac{e^x 6.105 rh}{100} \qquad (5.4.2)$$

rh is the atmosphere's relative humidity (in percent) and x is defined as

$$x = 25.22\frac{T-273.2}{T} - 5.31 \log_e\left(\frac{T}{273.2}\right) \qquad (5.4.3)$$

where

p = total atmospheric pressure (mb)
e = partial pressure due to water vapour (mb)
T = temperature (°K).

Atmospheric refractivity is measured in *N-units*. Close to the earth's surface is will typically range between 250 and 400 N-units.

As barometric pressure and the content of water vapour in the atmosphere decrease rapidly with altitude, while temperature decreases more slowly, the refraction index and refractivity also decrease, at increased altitudes.

Often, instead of refractivity, we consider a modified refractivity, which is useful to examine the refractivity gradients and their effect on radio propagation. It is defined as

$$M = N + 0.157\, h \qquad (5.4.4)$$

with height h expressed in metres and as

$$M = N + 0.048\, h \qquad (5.4.5)$$

for height h expressed in feet.

5.4.2 Effective earth radius

In free space, where the refraction index is constant, an electromagnetic wave travels as a straight line. In the earth's atmosphere, the speed of wave propagation is lower and the refraction index decreases for increased altitudes. For this reason, wave propagation no longer occurs in straight lines and waves are bent downwards. It is however convenient to view the refractive effects in terms of straight-line propagation. This can be done with good approximation considering a homogeneous atmosphere instead of the actual atmosphere and substituting the actual earth radius with an *effective earth radius* to correctly compute signal interaction with earth surface.

The *effective earth radius factor*, K, is defined as the factor to be multiplied by the actual earth radius a to obtain the effective earth radius a_e

$$a_e = Ka \tag{5.4.6}$$

K is bound to the refractivity gradient by the following equation:

$$K = \frac{1}{\left(1 - 10^{-6} a \frac{dN}{dz}\right)} = \frac{1}{\left(10^{-6} a \frac{dM}{dz}\right)} \tag{5.4.7}$$

where $\frac{dN}{dz}$ and $\frac{dM}{dz}$ are the gradients of N and m respectively and z is expressed in the same unit of measurement a.

The average earth radius is generally assumed as $6.371 \cdot 10^6$ m. From standard refraction conditions, where $\frac{dN}{dz} = -0.039$ N-units per m, equivalent to $\frac{dM}{dz} = 0.118$ M-units per meter, it results that $K \cong 1.33 \cong 4/3$.

Values of K lower than 1 identify downward refraction which *reduces* the propagation range. High values of K make over-the-horizon propagation possible.

K=2/3 is adopted instead of K=4/3 as "standard" earth radius [17]. This takes into account *subrefractive* conditions, which limit the maximum achievable range. The availability of detailed climatological information (Sect. 5.5) enables representation of propagation conditions conforming to conditions during system deployment.

Equation (5.1.1) can be modified as follows, to account for atmospheric refraction:

$$range_{refr} \cong 0.922(\sqrt{Kh_t} + \sqrt{Kh_r}) \tag{5.4.8}$$

where K is the effective earth radius factor. The result, as in the case of Eq. (5.1.1), in expressed in n.mi.

To measure the impact of the effective earth radius on line-of-sight radio transmission, let us apply Eq. (5.3.8) to the antenna heights used in our experiments (e.g. 8.7 m transmitting antenna on buoy, 33 m receiving antenna onboard NRV *Alliance*). Choosing K=2/3 instead of K=4/3 leads to a reduction of range of 2.7 n.mi (6.5 n.mi maximum range with K=2/3, 9.25 n.mi maximum range with K=4/3).

To compensate for this unfavourable value of K we would have to raise the buoy antenna to 21 m and the receiver antenna on NRV *Alliance* to 60 m, demonstrating the importance of accurate design, testing and modelling.

5.4.3 Equivalent refractivity gradient

One last consideration is devoted to the definition of G_e, the equivalent refractivity gradient, which is a key variable in the definition of K (Eq. 5.4.7). Because of atmospheric refraction, the *actual* propagation path is approximately an arc of a circle of radius r with curvature

$$\frac{1}{r} = -10^{-6} G_e \qquad (5.4.9)$$

where G_e is the *equivalent refractivity gradient.* G_e equals the mean value of the refractivity gradients $G = \frac{dN}{dh}$ encountered along the hop. The hop is a perfect arc when G is uniform all over the path.

It has been observed that G_e is a random variable that can be considered Gaussian on long hops. It has also been shown that on shorter hops, within the limit of 20 km (10.79 n.mi), the distribution of G_e coincides with G at an arbitrary point of the path, so that G can be used instead of G_e [8]. In our calculations we have adopted this approximation.

It must however be remembered that, while G can be assumed constant within a geographical area of a size comparable to the one we under consideration, it is also true that the characterization of G can vary substantially with time, in accordance with changed atmospheric parameters.

5.5 RF propagation models

In the post-cruise data analysis phase, extensive use was made of the Engineer's Refractive Effects Prediction System (EREPS) Version 3.0, distributed by SPAWARSYSCEN San Diego [7]. EREPS contains a database of meteorological and

environmental characteristics for most of the earth's surface. Using the EREPS-SDS program it is possible to retrieve parameters for a particular area of interest.

First, we illustrate the functionality of EREPS-SDS.

The user selects the appropriate geographic area (identified by Marsden squares, that is, squares the sides of which measure 10° of latitude and longitude), (Fig. 16).

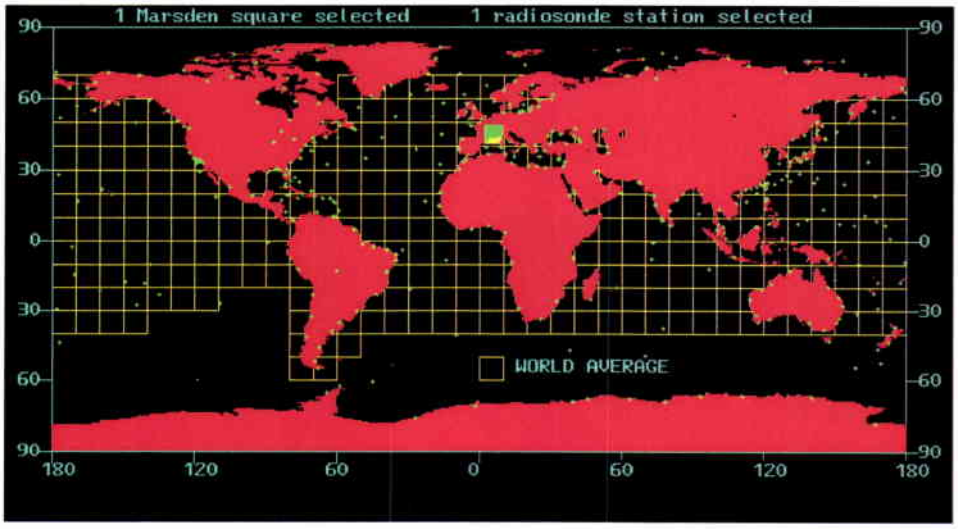

Figure 16 *EREPS SDS browser*

Next, a screen is displayed, summarizing the information of interest (Fig. 17):

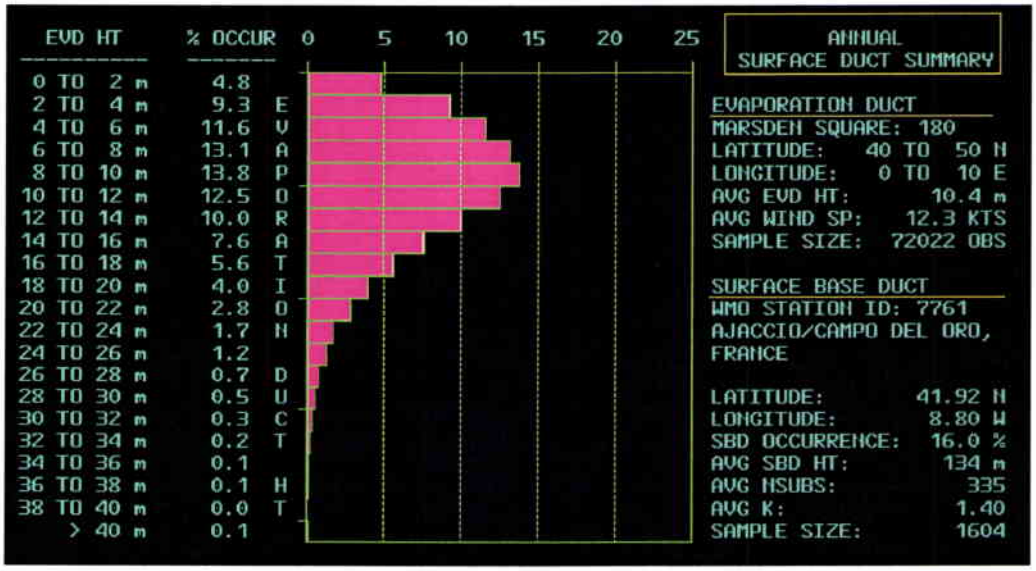

Figure 17 *Summary for DUSS 98 operations area*

It is possible to select more that one Marsden square at a time: EREPS-SDS will present average data for the areas that have been selected.

Using EREPS-SDS we have extracted the following statistical atmospheric parameters relative to the geographical area for DUSS 98:

Average wind speed (kn)	12.3
Average evaporation duct height (m)	10.4
Average surface based duct height (m)	134
Surface based duct statistical occurrence	16%
Average value of refractivity at surface	335
Average effective earth radius factor, K	1.4

Those parameters were fed to the EREPS suite of programs and served as a basis for our computer simulations.

5.6 Link-balance

The general form for a link-balance equation is

$$Link_{bal} = P_T + Tx_{gain} - L_T - N_T + Rx_{gain} - R_{thres} \qquad (5.6.1)$$

where:

$Link_{bal}$	Link-balance (dB)
P_T	Transmit power (dBm)
Tx_{gain}	Transmission antenna gain (dB), discussed in Sect. 5.2
L_T	Total path loss (dB), $L_T = L_G + L_M + L_S$
L_G	Signal attenuation (dB) due to geometrical spreading only, is a function of range and refraction conditions.
L_M	Loss factor accounting for signal attenuation and degradation due to multipath effects and signal smearing (dB)
L_S	Comprehensive system loss factor, accounting for signal attenuation and degradation due to antennae, antenna cables, amplifiers (dB)
N_T	Term accounting for ambient noise and receiver noise (dB)
Rx_{gain}	Receiver antenna gain (dB)
R_{thres}	Receiver sensitivity threshold (dB)

Link-balance is the result of the link-balance equation and is the measure of effectiveness of the communication system. The decision as to whether a communication system is capable of delivering the desired performance is made by comparing the link-balance to *receiver sensitivity*. Receiver sensitivity (often called *receiver threshold*) is the minimum signal-to-noise ratio required at receiver input to obtain the corresponding desired bit error rate (usually ranging from 10^{-6} to 10^{-9} for communication links). A positive link-balance quantifies the signal excess above the minimum threshold (in dB) and is a measure of the *robustness* of the communication to fluctuations of the conditions, e.g. if the excess is only of 2-3 dB, we can expect serious outage problems. Minimal additional interference will be sufficient to go below the threshold. On the other hand, a positive balance of 10 dB or more corresponds to a reliable system.

Transmission gain measures the gain of the transmitting antenna. Best performance would be obtained using high gain directive antennae on both sides of the connection. This is impractical, at least on the buoy side, where omnidirectional antennae in the horizontal plan are an almost mandatory choice.

5.6.1 Link balance: the propagation loss term

Total path loss includes the effect of the following components:

- Geometrical spreading of the signal wavefront, which reduces power flux density. Using an ideal omnidirectional antenna (isotropic radiator) it follows a spherical spreading pattern (Eq. 5.2.14)

- Evaporation ducts close to the sea surface (interactions between the lower atmosphere and sea surface)

- Comprehensive system loss, including attenuation and degradation on cable between antenna and receiver, pre-amplifier noise and signal degradation

- Multipath interference due to refraction of the transmitted signal off the troposphere (where applicable)

- Multipath interference due to reflection of the transmitted signal off the surface of the water

Total path loss has been calculated on the basis of the declared specifications of radio equipment using EREPS-PROPR (propagation *versus* range) model with the appropriate area-specific parameters, (Sect. 5.5). The effect of environmental parameters such as sea state and system parameters such as frequency and horizontal / vertical polarization on propagation loss has been carefully studied:

Annex B lists the results of EREPS-PROPR for the 2.28 GHz link.

Annex C lists the results for the 400 MHz link.

In Annex B we observe several propagation *nulls*, that is, areas where propagation loss shows a sharp increase. Two such nulls can be measured at 0.6 and 1.4 n.mi from a transmitter 6 m above the sea level / receiver at 26 m.

Antennae with horizontal polarization are considered first. In the absence of wind (Fig. B.1), nulls exceed 50 dB, compared to free space propagation loss, where no multipath nulls occur. If the wind increases to 10 kn (Fig. B.3), a normal condition for the area of our experiment, the propagation loss nulls are less pronounced, (30-35 dB) due to non perfectly specular reflections on the sea surface (increased roughness). If wind conditions rise to 20 kn (Fig. B.5), the nulls are limited to 10-15 dB, in comparison to free space. These results are consistent with the theory illustrated in Sect. 5.3.

In the case of antennae with vertical polarization, only one propagation null is detectable, at 1.4 n.mi: in conditions of absence of wind (Fig. B.6), the null is 10 dB below free space, 5 orders of magnitude less than horizontal polarization. As wind increases, vertically polarized antennae show even lesser nulls (Fig. B.7).

At the maximum range of 10 n.mi, horizontal and vertical polarizations offer a similar behaviour, irrespective of wind conditions.

Similar remarks hold for Annex C (400 MHz). Multipath nulls are concentrated at very short range (less than 1 n.mi) and nearly disappear when wind speed increases from zero to realistic values. Free space propagation loss at 10 n.mi is lower at 400 MHz than at 2.28 GHz (110 dB *versus* 124 dB). However, when interactions with the sea surface are also considered, losses increase to 125 dB (400 MHz) *versus* 130 dB (2 GHz) (with little dependence on sea surface conditions).

Vertical polarization offers better performance than horizontal polarization, especially in conditions of low winds. With stronger winds both horizontal and vertical polarization offer good performance.

The lower frequency offers less propagation loss, although the effects of the sea surface, simulated by AREPS / EREPS, reduce the advantage to 5 dB only. Nulls at 400 MHz are less relevant and occur at shorter range.

5.7 Comparison between computer models and measured data: 400 MHz

In this section the link-balance (Eq. 5.6.1) (computed with Eq. (5.2.14) or EREPS-PROPR) is compared with the real data measured during the DUSS 98 cruise, for the 400 MHz communication system.

The system parameters of the 400 MHz link are:

TX power	43 dBm (20 W)
TX antenna gain	4 dB
RX antenna gain	3.2 dB
Cable loss between antenna and receiver	4 dB
System loss	4 dBm
Pre-amplifier gain	12 dB

The receiver was positioned onboard NRV *Alliance*, with the antenna 26 m above sea level. The transmitter was positioned either on the DUSS buoy (6 m) and subsequently onboard ITS *Ponza*, with a higher antenna mast (13.7 m).

Propagation loss for the on-buoy antenna (6 m):

Range (n. mi)	**EREPS** Propagation loss (dB) (wind = 12.3 kn)	**Free space loss** (dB)
0.41	80	82
0.6	84	85
0.8	87	88
1	90	90
1.5	96	93
2	101	95
2.5	104	97
3	106	99
3.5	108	99
4	110	100
4.5	112	103
5	113	103
5.5	115	104
6	116	105
6.5	117	106
7	119	106
7.5	120	107
8	121	107
8.5	122	108
9	123	108
9.5	124	109
10	126	109

Propagation loss for the antenna onboard ITS *Ponza* (13.7 m) (6 dB better at 10 n.mi):

Range (n. mi)	**EREPS** Propagation loss (dB) (wind = 12.3 kn)	**Free space loss** (dB)
0.41	84	82
0.6	84	85
0.8	84	88
1	85	90
1.5	90	93
2	94	95
2.5	98	97
3	101	99
3.5	103	99
4	106	100
4.5	108	103
5	109	103
5.5	110	104
6	112	105
6.5	113	106
7	114	106
7.5	115	107
8	116	107
8.5	118	108
9	119	108
9.5	120	109
10	120	109

The following figures summarize the link-balance for three cases: free space propagation, propagation simulated in a marine environment and real data collected during the experiment.

The horizontal axis represents the transmission range in n.mi. The vertical axis represents the link-balance at the receiver, expressed in dB and accounting for all effects, including receiver electronic noise.

EREPS balance indicates the link-balance computed using propagation loss data modelled by EREPS, accounting for environmental parameters such as sea state or atmospheric conditions.

Theor balance indicates the link-balance calculated using free space propagation loss.

Actual measure illustrates the link-balance based on data measured during the experiment.

Threshold indicates the receiver sensitivity: as long as link-balance is higher than the receiver threshold, the communication system is effective.

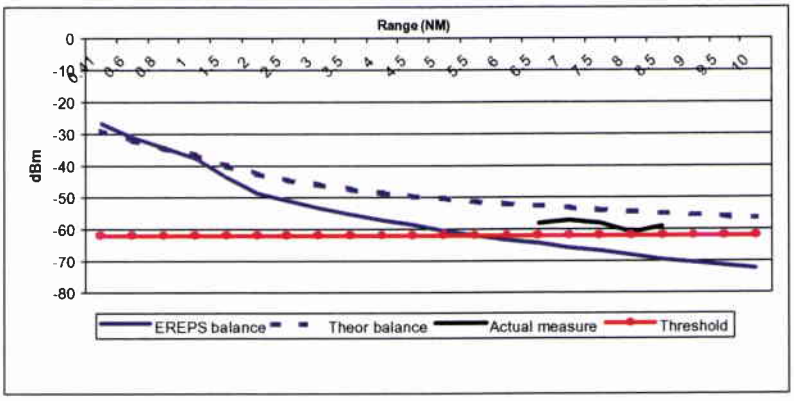

Figure 19 *400 MHz system - Comparison of data measured at the receiver with computer predictions (free space loss, loss accounting for atmospheric conditions, calculated using EREPS). Transmitter on buoy (6 m), receiver onboard NRV Alliance (26 m)*

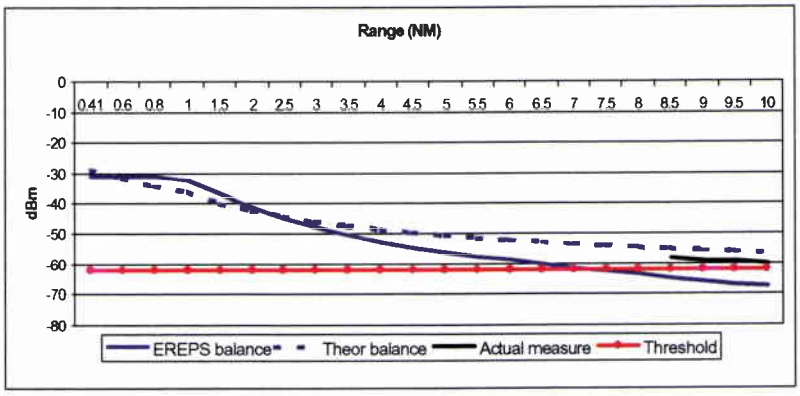

Figure 20 *400 MHz system - Comparison of data measured at the receiver with computer predictions (free space loss, loss accounting for atmospheric conditions, calculated using EREPS). Transmitter on ITS Ponza (13.7 m), receiver on NRV Alliance (26 m)*

The offset between free space propagation loss (dotted blue line) and the EREPS propagation loss prediction (blue line) is a consequence of more accurate modelling of multipath and atmospheric attenuation. Atmospheric data were extracted from the EREPS-SDS database of environmental information.

The agreement of predicted data with measurements demonstrates that propagation models can be used to successfully predict the behavior of a radio frequency link. The model is pessimistic, by comparison to experimental data. The offset between measured data and computer predictions (ranging between 5 and 10 dB) is reasonable and is usually included in the term for system loss, L_s.

More accurate environmental measurements (sea surface temperature, atmospheric temperature, humidity, wind speed) during the radio transmission tests, may lead to improvements of model accuracy.

The experimental threshold was found to be around –62 dB, with a very rapid degradation of link quality. The experimental data show that 7 more metres of transmitter antenna can increase range by 3 miles of range. Looking into simulated propagation loss data we find that this corresponds to 6 more dB into the link balance. The same result can therefore be achieved by modifying other terms, such as transmitter power, receiver antenna gain and receiver threshold. This would be done at the expense of such system parameters as battery duration / size, link stability (narrow antenna beams in a buoy – ship link), data throughput. Moreover, experimental data also show that the lower antenna is associated with larger signal fluctuations, which affect throughput, reliability and protocol complexity of the link.

5.8 Comparison between computer models and measured data: 2.28 GHz

In this section we apply the same methods of Sect. 5.7 to measurements at 2.28 GHz. Detailed plots of experimental data are presented in Sect. 4 (Figs. 1, 2 and 3). The system parameters of the 2.28 GHz link are:

TX power	38 dBm (6 W)
TX antenna gain	0 dB
RX antenna gain	22 dB
Cable loss between antenna and receiver	6 dB
System loss	4 dB
Pre-amplifier gain	18 dB

The receiver was onboard NRV *Alliance*, with antenna 33 m above sea level. The transmitter was positioned onboard ITS *Ponza*, with an 8.7 m antenna mast.

Figure 21 provides a summary for link-balance at the receiver in the three cases considered (including such effects as receiver electronic noise): free space propagation, propagation in a realistic marine environment, experimental measurements.

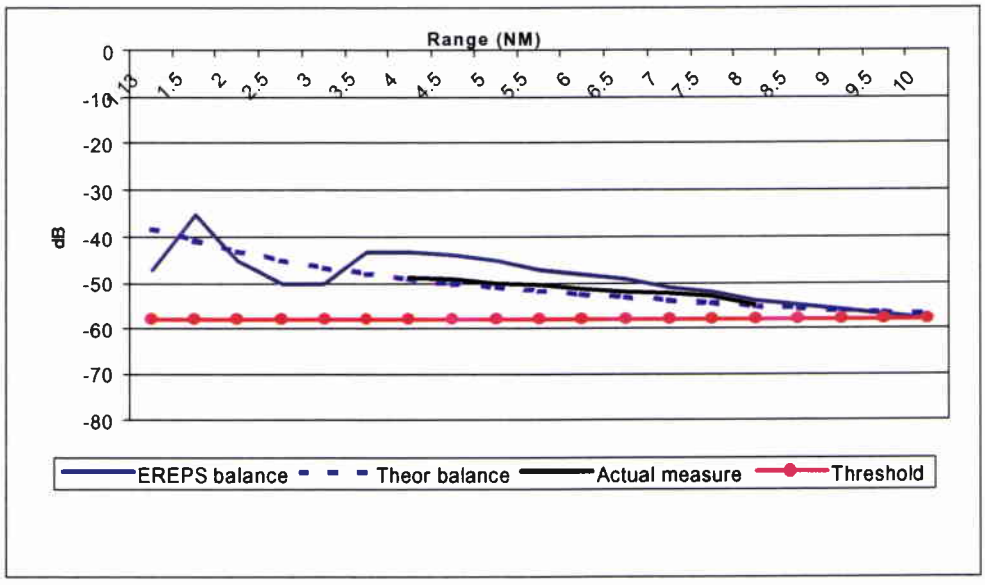

Figure 21 *2.28 GHz system - Comparison of data measured at the receiver with computer predictions (free space loss, loss accounting for atmospheric conditions, calculated using EREPS). Transmitter on ITS Ponza (8.7 m), receiver on NRV Alliance (33 m directional antenna).*

Good agreement between experimental data and models is achieved. The experimental threshold is close to the nominal one. Although this system uses a less powerful transmitter (6 W instead of 20 W for the 400 MHz system), performance is satisfactory up to the range of 8 n.mi with the existing 6 m antenna. In order to obtain 10 n.mi from the DUSS buoy, it is necessary to increase antenna height from 6 m to 8.7 m. This corresponds to a signal level increase of 4 – 5 dB, as confirmed by the model (see also Fig. 12). Additional margins could be obtained by the fine tuning of other parameters such as transmitter power and antenna gains. However, this involves larger costs for RF equipment than the 400 MHz link.

5.9 Comparison of propagation loss at 400 MHz and 2.28 GHz

We can compare the theoretical propagation loss for the two candidate channels: 400 MHz and 2.28 (or 2.4) GHz. The first result is that radio propagation in the 2-GHz frequency range presents an increase in propagation loss of 15 dB, by comparison with propagation at the frequency of 400 MHz, (Fig. 22). We assume transmission from the DUSS buoy (6 m antenna). This increase is clearly justified by the free-space propagation loss Eq. (5.2.13), which defines the relationship between signal attenuation and radio frequency. The difference between the 2.28 and 2.4 GHz channels proves to be minimal.

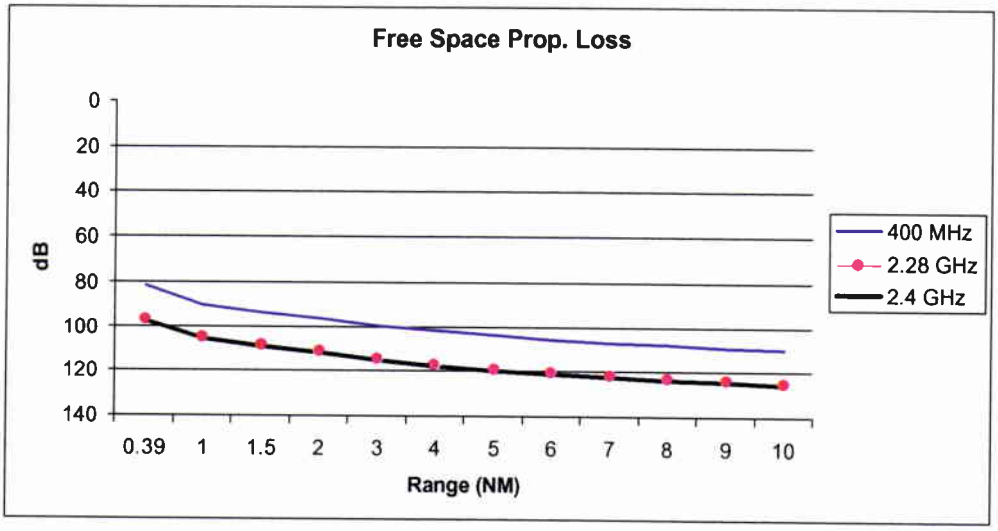

Figure 22 *Comparison of propagation loss at different frequencies, using Eq. (5.2.13)*

This observation is not sufficient to determine whether one channel is better than the other.

The lower the frequency, the more difficult it is to receive a radio signal from an antenna close to the sea surface (Figs. 11 and 13), because the elevation angle of the lowest interference lobe is

$$\frac{\lambda}{4h} \qquad (5.9.1)$$

where λ is wavelength and h in antenna height (both expressed in metres).

Parameters such as wind speed and sea state play an important role in conditioning the entity of propagation loss. We have conducted comparative measures to assess the quantitative effect of those parameters on propagation loss. Our principal aim was to estimate whether both channels were equally vulnerable to environmental and atmospheric effects or if, instead, one channel offered better performance than the other.

In Fig. 23 we compare propagation loss in the two channels, considering the same environmental parameters.

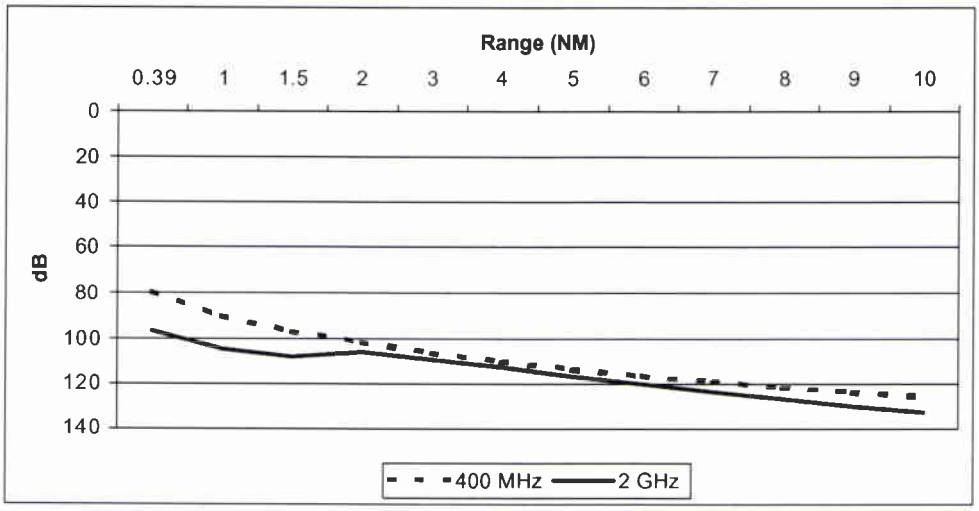

Figure 23 *Comparison of propagation loss at 400 MHz and 2 GHz, accounting for environmental effects (atmosphere, sea state) on radio propagation*

For both channels, Fig. 24 illustrates the difference in signal attenuation between free space propagation and propagation accounting for environmental effects, modelled using EREPS-PROPR, assuming standard wind conditions of 12 kn. Antenna height is 6 m.

The vertical scale measures the difference, in dB, while the horizontal axis shows the range in n.mi.

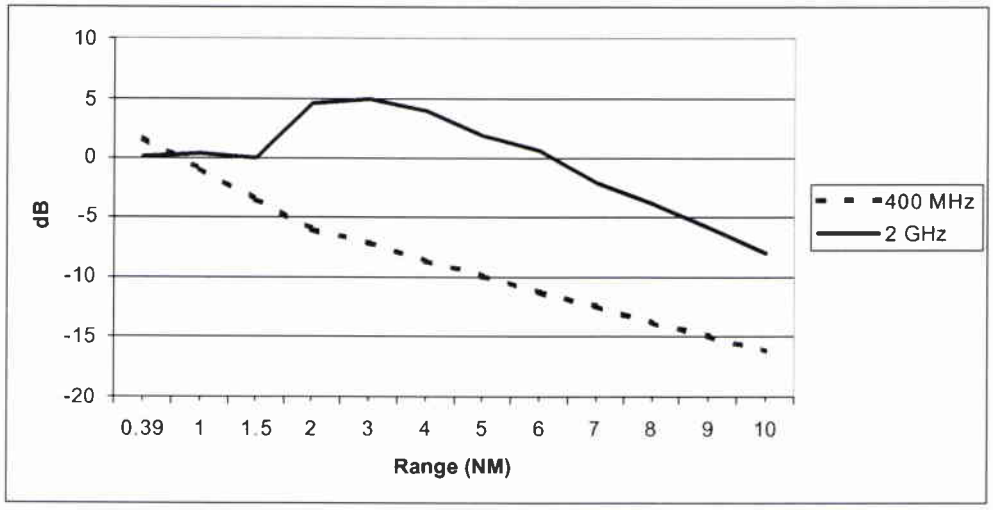

Figure 24 *Difference between realistic propagation loss in the marine environment and free space propagation, as a function of range*

Observing the distance of the two graphs from the *zero* reference value of the Y-axis, which marks the offset from free space propagation, it is clear that the 2 GHz channel is less influenced by sea state and wind speed.

It is also clear that the impact of environmental factors on the 400 MHz channel is *negative* and that the adverse effects increase as a function of range.

The 2 GHz channel seems to benefit from environmental factors. The improvement by comparison to free space propagation reaches the maximum value of 5 dB in the 2-3 n.mi range. Positive effects are measured up to a range of 6 n.mi.

Continuing the comparison with free space propagation, we notice that, at the maximum range of 10 n.mi, interaction with the sea surface increases propagation loss by 8 dB and 16 dB for 2 GHz and 400 MHz, respectively.

5.10 Summary of results for the 400 MHz and 2.28 GHz systems

The basic theory of radio propagation has been reviewed up to the definition of link-balance equations as a tool to analyze experimental results and effectively compare the performance of different systems. The effects of interactions with sea surface, wind state and antenna height were also illustrated by means of specific models.

Results:

- The objective range of 10 n.mi is achieved by both systems with different characteristics.
- All configurations require a directional receiver antenna positioned onboard NRV *Alliance*.
- The 2.28 GHz link provided the desired 10 n.mi range with transmitting antenna heights of 8.7 m (ITS *Ponza*) and a directional receiving antenna. Some minor instability has been observed at short range (around 3 n.mi). The link was stable up to the range of 8 n.mi. Subsequent transmission was subject to higher outage probability, but within acceptable limits.
- The 400 MHz link was successfully tested at ranges of up to 10 n.mi with a 13.7 m antenna on ITS *Ponza* and 7 n.mi with the existing 6 m high buoy. A decrease of transmit power would lead to longer operation of the battery-powered DUSS buoys: our tests show that a maximum range of 5 n.mi was achieved with 4.5 W transmit power (instead of 20 W) and a 13.7 m tall transmitter.
- With the same transmitter height of 6 m, the 2.28 GHz link at 10 n.mi is affected by more propagation loss than the one at 400 MHz (+15 dB in free space, +5 dB with accurate model of the sea surface).

- At 2.28 GHz it is possible to use a lower antenna mast, according to Eq. (5.9.1). A taller mast and higher transmission power are required at 400 MHz.

- Both links are successfully modelled by link-balance equations, which permit insight into the trade-offs relating the various engineering parameters (e.g. frequency, transmission power, antenna gain, antenna height).

- AREPS propagation model faithfully simulates the experimental propagation conditions due to careful consideration of environmental factors.

- The 2.28 GHz link is subject to deeper nulls at short range (around 3 n.mi range). Figs. 21, 1 and 3 show correspondence between measured data and the link-balance model. The 400 MHz link shows better stability at short range than the 2.28 GHz link.

- The equipment used during the experiment represents optimal engineering trade-offs and economic considerations.

To summarize:

1. We express link-balance terms in dBm measured at the receiver input. The receiver threshold, therefore, includes the noise terms.

2. Noise is mostly due to electronic equipment (electronic noise) and its effect is visible as variations of the receiver threshold which reduce the expected pre-amp gain.

3. System loss L_s is 4 dB at 400 MHz and 10 dB at 2.28 GHz. Those figures are an estimate and agree with measured data.

4. The empirical threshold is –62 dBm for the 400 MHz system and –58 dBm for the 2.28 GHz system. Since the performance of the two systems is roughly equal (at the limit of 10 n.mi), also the corresponding balance equations are equal.

5. Analysis of link-balance terms leads to useful comparisons of the two systems, listed in the following table.

400 MHz	*2.28 GHZ*
has a higher transmit power **+ 5 dB**	
	has a higher gain at the receiver antenna **+ 16 dB**
has a higher gain at the transmit antenna **+4 dB**	
has a lower cable loss **+ 2 dB**	
	has a higher amplifier gain **+6 dB**
has a lower propagation loss **+11 dB**	
Total ***+22 dB***	***+22 dB***

The 2.28 GHz system has a propagation loss disadvantage of 11 dB with respect to the 400 MHz system: during the experiment, a higher mast was used at 400 MHz than at 2.28 GHz (13.7 m instead of 8.7) Propagation loss is 5 dB higher than at 400 MHz when masts of equal height (6 m) are used.

The 2.28 GHz system can be further improved by increasing transmit power and transmit antenna gain: the expected result will be a BER improvement at the 10 n.mi range, leading also to a lower outage probability.

The 400 MHz system can benefit from improvements of receiving antenna directivity. These would imply a larger size (due to wavelength), but would permit some savings on mast height (very critical) and battery capacity.

6. It is important to improve engineering factors in order to increase the link-balance margin at the range of 10 n.mi, which will lead to a more dependable system. Further improvements can be obtained through the adoption of more efficient modulation and coding schemes. Such topics will be covered in a future report.

Additional conclusions are presented in Sect. 7.

6

Fighting noise and multipath interference

This section presents notes on the major factors which adversely affect radio link performance close to the sea surface (apart from plain propagation loss, addressed above): noise and multipath. It also reviews codes and modulation techniques envisaged to counter such effects.

6.1 Noise

Noise is introduced by different sources: both natural (earth and atmosphere) and artificial (electronic noise in the receiver and in RF amplifiers). The receiving antenna collects noise emissions from galactic, solar and terrestrial sources, which constitute the sky background noise. The sky background noise appears as a combination of galactic effects that decrease with frequency and atmospheric effects that become significant at frequencies higher than 10 GHz. For this reason, communication in the 2 GHz frequency range will be less affected by sky background noise than the 400 MHz counterpart [14].

An in-depth discussion on noise goes beyond the purpose of this document. We will however keep in mind an important result of Shannon's Mathematical Theory of Communication :

"*If the rate of information from the source does not exceed the capacity of a communication channel, then there exists a coding technique such that the information can be transmitted over the channel with an arbitrarily small frequency of errors, despite the presence of noise*" [9]

The coding strategy that can be implemented depends on link architecture. For a full duplex channel, it will be possible to request the retransmission of information containing detected errors using *automatic repeat request* (ARQ). In our case, where the link is monodirectional, or, at most, strongly asymmetric, error control must take place through *forward error correction* (FEC) [9].

No matter what coding strategy is used, it is going to have an impact on the global throughput of the system. Adding processing capabilities to the DUSS buoys would decrease the data rate requirements, thus increasing significantly the overall reliability of the system.

6.2 Fading caused by multipath interference

The other main source of interference is introduced by multipath effects (Sect. 5.3). As a consequence of multipath, the shipboard antenna receives a large number, say N, of reflected and scattered waves. Because of wave cancellation effects, the instantaneous received power measured at the receiving antenna can be assimilated to a random variable, dependent from environmental conditions and relative positions of transmitter and receiver. The random variable can be characterized by a Rayleigh distribution [10]. When a strong and dominant component is measured, as in some LOS systems, the distribution is better modelled using a Rician distribution.

Multipath scattering can have adverse effects on digital wireless communication systems. The following figure, generated using the EREPS-RAYS program, depicts the ray tracing of electromagnetic waves radiating from a generic buoy with an antenna height of 6 m.

If the receiver antenna is positioned at any of the points in which two or more rays intersect, the receiver will be affected by multipath. Intensity of the reflected ray and phase reversals will be a function of sea roughness and frequency.

Reflections from the buoy structure are not taken in consideration.

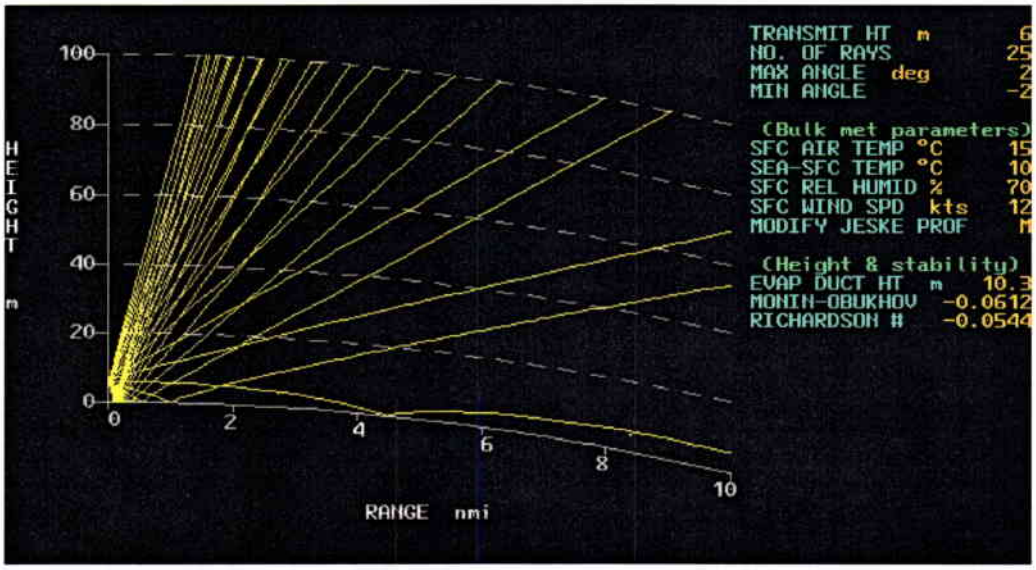

Figure 18 *Ray tracing from a generic buoy as a function of transmission range.*

6.2.1 Word error rate and probability of bit error

In a system subject to Rayleigh fading, the received modulated signal power fluctuates over a large range, typically 10 dB to 50 dB. A system such as the one we are studying, where communication takes place between at-sea platforms, can be characterized as *slow-Rayleigh fading*. The duration of the fades is long: this implies that the bit error rate and the corresponding word error rate will be high for longer periods of time, that is, for long burst durations.

Fading is also influenced by relative motion of the transmitter and of the receiver: this motion is a function of sea state, which results in *Doppler spread*, that is, a time-based variation of received signal phase. Movements greater that a few hundredths of wavelengths are sufficient to induce signal fluctuations. In our case, for the 400 MHz system we have a wavelength of 75 cm, which is reduced to 13 cm for the 2.28 GHz system. This means that Doppler spread takes place if the receiver (or transmitter) is moving over a range of only 7.5 cm or 1.3 cm respectively. It appears that the 400 MHz is more resistant to Doppler effects. This is true with identical antennas masts: however, the 400 MHz system requires a taller mast, so that the advantage to be minimal, the two frequencies are therefore comparable with respect to Doppler spread.

Several techniques have been proposed to improve system resistance to multipath: some of them, such as antenna (spatial) diversity, are of difficult implementation, given the restrictions imposed by operating from a buoy. Other techniques, such as spread-spectrum or multi-carrier modulations, may prove to be of extreme interest.

Probability of bit error is also influenced by the modulation that is adopted for the communication link. It is well known that different modulations present different characteristics with respect to spectral and power efficiency: additional studies should be conducted to assess the impact of different modulations on the performance of DUSS radio links.

6.3 Spread-spectrum and multi-carrier modulations

Important performance improvements could derive from the adoption of spread-spectrum techniques in the implementation of the wireless link.

Spread-spectrum systems have been widely studied since the mid-1950's for military anti-jamming tactical applications and anti-multipath communications. In spread-spectrum systems the signal occupies a bandwidth in excess of the minimum necessary to send the information: the band spread in accomplished by means of a code which is independent of the data and a synchronized reception with the code is used for despreading and subsequent data recovery [11].

Spread-spectrum systems are implemented using two main techniques, termed *direct-sequence* and *frequency-hopping*. Direct-sequence generation is made using a fast pseudo random sequence which causes phase transitions in the carrier containing data.

Frequency-hopping, instead, uses a pseudo random pattern to shift the carrier several times a second.

Resistance to multipath is achieved through different mechanisms. In direct-sequence the interference is *attenuated* and its effect is made less destructive, while in frequency-hopping the system will switch to a new frequency before the reflected (delayed) ray is able to reach the receiver. This last technique is called *interference avoidance*. Both techniques also exhibit a certain tolerance to jamming.

We could also counter multipath by using multi-carrier modulations. The US Navy is developing a prototype naval communication system based on Orthogonal Frequency Division Multiplexing (OFDM). This multi-carrier modulation is expected to provide efficient bandwidth utilization and good performance in presence of multipath. Such a system will make possible an efficient exploitation of existing communication channels in the 250-400 MHz frequency band.

However, it is our opinion that, in an operational system, where multipath resistance is to be associated to low probability of intercept and jam-resistance, the only option will be to adopt spread-spectrum transmission.

A test of an alternative wireless link, implemented using spread-spectrum equipment, is illustrated in Annex D.

A complete overview of spread-spectrum communications theory is given in [12] and [16].

7 Conclusions

The experiments and analysis result in the following conclusions:

- The feasibility of a 10 n.mi. 2 Mbps simplex radio link was proven at both 400 MHz and 2.28 GHz.
- The chosen digital code (Biphase-Mark) and the telemetry link scheme selected for the DUSS prototype were successfully tested and confirmed.
- Accurate modelling of radio link performance by the means of link-balance equations and radio propagation simulators (AREPS and EREPS) is possible.

  •The most critical elements of the system are:

  - Transmitter antenna height, on the buoy side
  - Transmitted power
  - Receiver antenna height and directivity, on the ship side

  The above factors strongly affect performance, size, cost, complexity and deployment constraints. Valuable information was collected about such tradeoffs, which can be utilized in the design of the new prototype system.
- The 400 MHz link offers a lower propagation loss than the 2.28 GHz link (5 dB less for masts of equal height, 11 dB less in the experiment).
- The 2.28 GHz frequency band is less sensitive to background noise and to interactions with the marine environment (e.g. multipath interference). For this reason, it is will be possible to deploy it in a wider range of operational and environmental conditions.
- The 2.28 GHz system used 6 W transmit power with an antenna height of 8.7 m and a receiver antenna height of 33 m. The 400 MHz used higher transmit power (20 W) and a higher antenna mast on the buoy side. 400 MHz equipment (in particular, RF amplifiers) is significantly less expensive.
- The two systems present a comparable link balance. The 400 MHz system presents a better BER at 10 n.mi. However, performance of the 2.28 GHz link at 10 n.mi is still compatible with sonar research operations (BER better than $3 \cdot 10^{-3}$).

- Antenna height on the DUSS buoy is a critical issue. Better results will be achieved with higher antenna masts: it will be necessary to assess the impact of a higher mast on the buoy geometry and mechanical structure. The objective height is of 9 m.

- Antennae with vertical polarization are superior to horizontal polarization.

- Buoy characteristics mandate the adoption of omnidirectional antennae on the buoy side. Directional antennae on the receiver side are necessary to make the link reliable. An open loop telemetry tracking system can be set up onboard NRV *Alliance* using onboard GPS and gyro information, thus relieving technical support personnel from an additional task during experiments. An extension of the existing mast on NRV *Alliance* above the existing 26 m, with adequate support for directional antennae, might be considered.

- A relaxation of range requirements to 6-7 n.mi permits use of the existing well tested radio buoy (with a 6 m high antenna mast). This would also considerably reduce deployment and handling constraints.

- The specification of 10 n.mi involves careful investigation into balloon and "kite" technology, deployed either from the buoy, or from the ship. The latter option entails additional concerns about mechanical interference with existing ship structures and enhanced sensitivity to unwanted signal sources.

- Alternately, a fixed, elevated relay station on the coast can also provide enhanced ranges. A similar setup has already been demonstrated in [13]. This option is relevant only for experimental applications. In an operational system, assuming air superiority, the same performance could be obtained by an aircraft station (e.g. ASW helicopter).

- The concept of repeater buoy to extend the maximum operational range deserves serious consideration and study. The measurements collected with a short omnidirectional antenna are representative of the achievable performance (8 n.mi range).

- The analysis of link balance shows space for improvements in the receiver antenna gain and receiver sensitivity (threshold) at 400 MHz and in the transmit power / transmit antenna gain at 2.28 GHz.

- Estimated system loss values lead to the conclusion that also improvements of pre-amplifier electronic noise can be profitably investigated.

- The same experiments were repeated with a spread-spectrum system at 128 kbps with only 0.6 W of transmitter power. The characteristics of resistance to hostile jamming and its low probability of intercept will be examined further in another study.

- Interesting data were collected about signal and error statistics up to the maximum operational ranges. This information, susceptible to improvement when the full data acquisition prototype is ready, is very useful in the selection of encoding schemes.

8

Recommendations and future activities

Further work is recommended on the following key subjects:

- Physical radio link

  Spread-spectrum techniques and other signal modulation and coding schemes deserve serious attention. Their interaction with the peculiar environment of the present application (air-sea boundary) may result in significant improvements to system performance and reliability. The concept of a "repeater" buoy is also promising, in the attempt to align radio ranges to acoustic performance.

- Operational issues

  Issues such as covert transmission, resistance to man-made interference and hostile jamming are vital to the application of radio links (with all their flexibility and advantages) to a potentially operational DUSS.

- Networks

  DUSS are a distributed, networked concept, presenting many interesting similarities with communication networks. DUSS can therefore benefit from a transfer of knowledge and techniques not only for data transport, but also for deployment schemes, operational principles and fusion of acoustic contacts. In particular the adoption of packet-switching network techniques such as Code Division Multiple Access (CDMA) or Collision Sense Multiple Access (CSMA) would enhance the overall system coordination and capabilities, implementing a real state-of-the-art distributed surveillance network.

- Satellite

  In-buoy processing and detection capabilities would also reduce traffic, making it reasonable to conduct tests with a satellite radio link. Modern routing protocols would further optimize data transfer requirements.

Acknowledgements

We thank the Captain and crew of ITS *Ponza* and NRV *Alliance* for their support. Valuable assistance was provided by the SACLANTCEN Engineering Technology Department and in particular by Mr Chiappini, Mr Chiarabini and Mr Lorenzelli.

References

[1] Mozzone, L., Bongi, S. Deployable Underwater Surveillance Systems - analysis of experimental results. SACLANTCEN SR-278. La Spezia, Italy, NATO SACLANT Undersea Research Centre, 1997.

[2] Mozzone, L., Bongi, S., Primo, F., Deployable Underwater Surveillance Systems - analysis of experimental results. Part II. SACLANTCEN SR-283. La Spezia, Italy, NATO SACLANT Undersea Research Centre, 1998.

[3] Mozzone, L., Bongi, S., Deployable Underwater Surveillance Systems - analysis of experimental results. Part III. SACLANTCEN SR-288. La Spezia, Italy, NATO SACLANT Undersea Research Centre, 1998.

[4] Mozzone, L., Bongi, S., Deployable Underwater Surveillance Systems. Localization and fusion of multistatic contacts. Evaluation of feasibility using experimental data. SACLANTCEN SR-291. La Spezia, Italy, NATO SACLANT Undersea Research Centre, 1998.

[5] Mozzone, L., Bongi, S. Localization and fusion of echoes with deployable multistatic active sonar: evaluation of feasibility using experimental data. ECUA'98 Fourth European Conference on Underwater Acoustics, Roma, 1998.

[6] Patterson, W.L. Advanced Refractive Effects Prediction System (AREPS) Version 1.0 User's Manual, TD 3028, San Diego, CA, Space and Naval Warfare Systems Center, 1998

[7] Patterson, W.L., Hattan, C.P., Lindem G.E., Paulus, R.A., Hitney, H.V., Anderson, K.D., Barrios, A.E., Engineer's Refractive Effects Prediction system (EREPS) Version 3.0, TD-2648. San Diego, CA, United States, Naval Command, Control and Ocean Surveillance Center (NCCOSC) RDT&E Division, 1994.

[8] Mojoli L.F., Mengali U., Propagation in line of sight radio links, Supplement to *Telettra Review* No. 37, 1985.

[9] Carlson, A.B., Communication systems, McGraw-Hill, 1986 [ISBN 0-07-100560-9].

[10] Papoulis, A., Probability, Random Variables and Stochastic Processes, McGraw-Hill, 1991 [ISBN 0-07-048477-5].

[11] Scholtz, R.A., The origins of spread-spectrum communications, *IEEE Transactions on Communications,* **30**, 1982:822-854.

[12] Pickholtz, R.L., Schilling, D.L., Milstein, L.B., Theory of spread-spectrum communications - a tutorial, *IEEE Transactions on Communications*, **30**, 1985: 855-884.

[13] Berni, A., Madrignani, L., Trangeled, A. Improvements to data networks in support of REA during Generic Oceanographic Array Technology (GOATS) 98, SACLANTCEN SM-336. La Spezia, Italy, NATO SACLANT Undersea Research Centre, 1998.

[14] Sklar, B. Digital Communications, Fundamentals and Applications, Prentice Hall, 1988 [ISBN 0-13-211939-0].

[15] Skolnik, M.I., Introduction to Radar Systems, McGraw-Hill [ISBN 0-07-057909-1].

[16] Conticello, C., Spread spectrum communications: an overview, *Alta Frequenza*, 1987, **61**: pp. 255-264.

[17] Fink, D.G., Electronics Engineers Handbook, McGraw-Hill, 1975 [ISBN 0-07-020980-4].

[18] Feher, K., Wireless Digital Communications, Prentice-Hall, 1995 [ISBN 0-13-098617-8].

Annex A – Pictures of assets and instruments

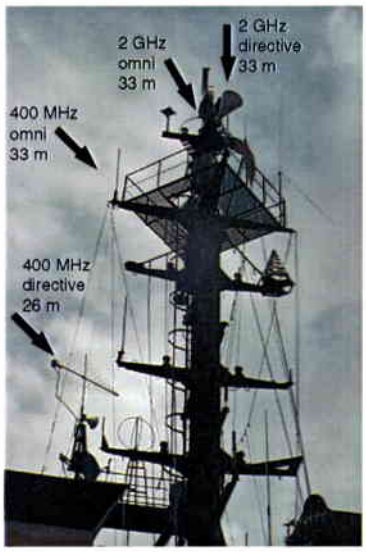

NRV Alliance antenna mast

Buoy - to - buoy link simulation

400 MHz buoy

Bit Error Rate measurement

ITS Ponza

2 GHz antenna on Ponza

400 MHz antenna on Ponza

Lab on Ponza

Annex B – Effect of Sea State on RF propagation: 2.28 GHz

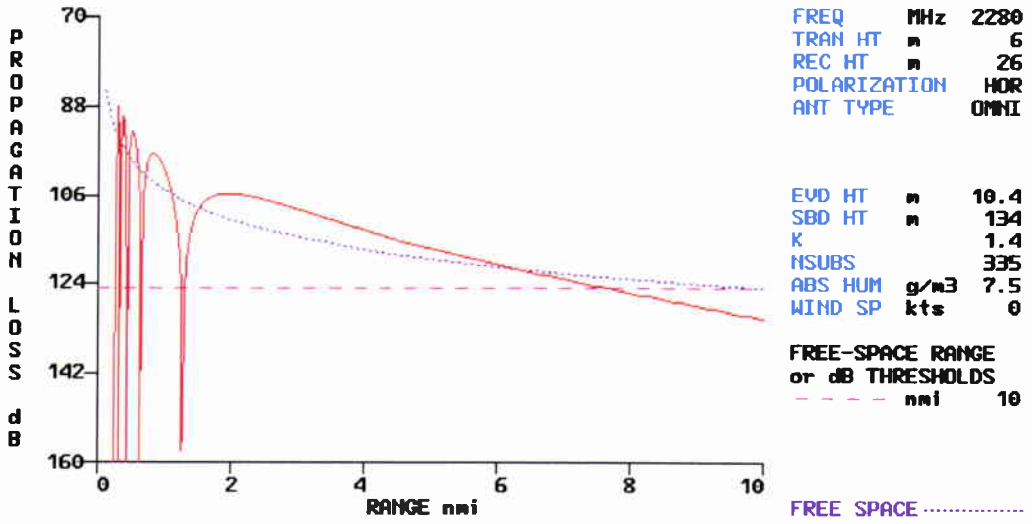

Figure B.1 *Propagation loss for test area: absence of wind, horizontal polarization.*

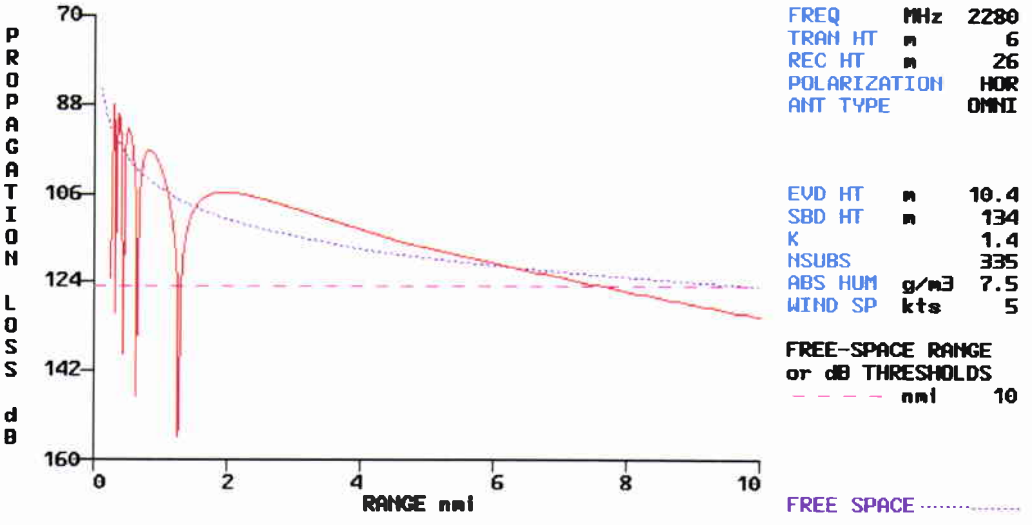

Figure B.2 *Propagation loss for test area: wind 5 kn, horizontal polarization.*

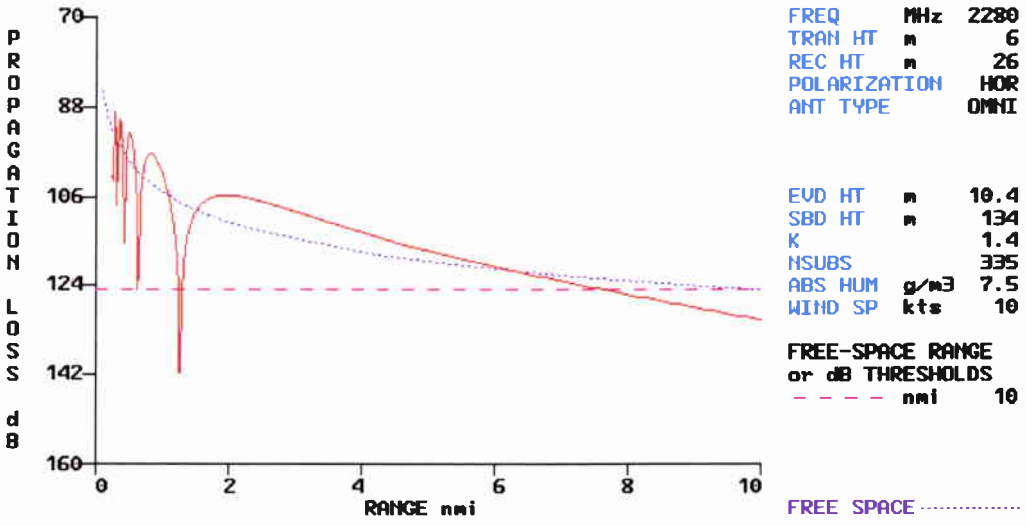

Figure B.3 *Propagation loss for test area: wind 10 kn, horizontal polarization.*

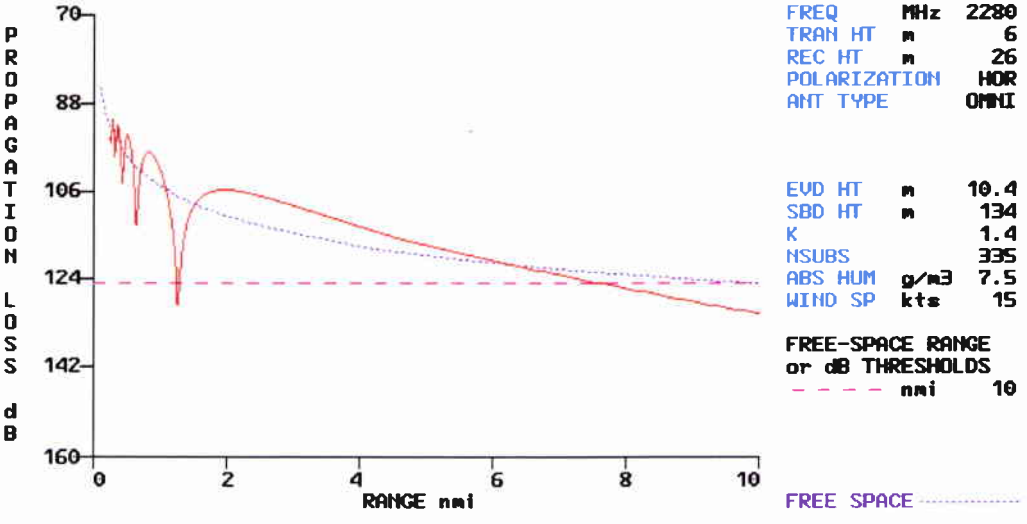

Figure B.4 *Propagation loss for test area: wind 15 kn, horizontal polarization.*

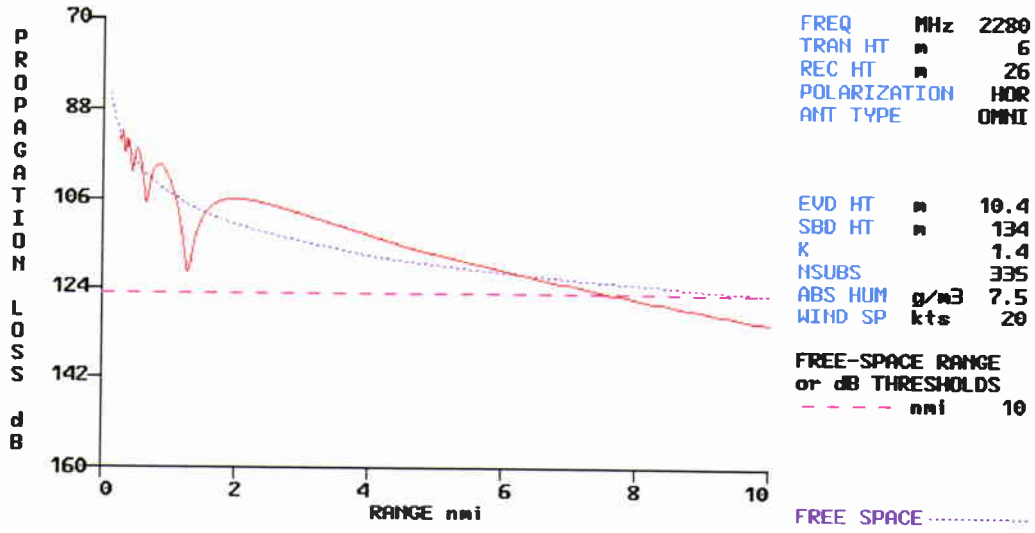

Figure B.5 *Propagation loss for test area: wind 20 kn, horizontal polarization.*

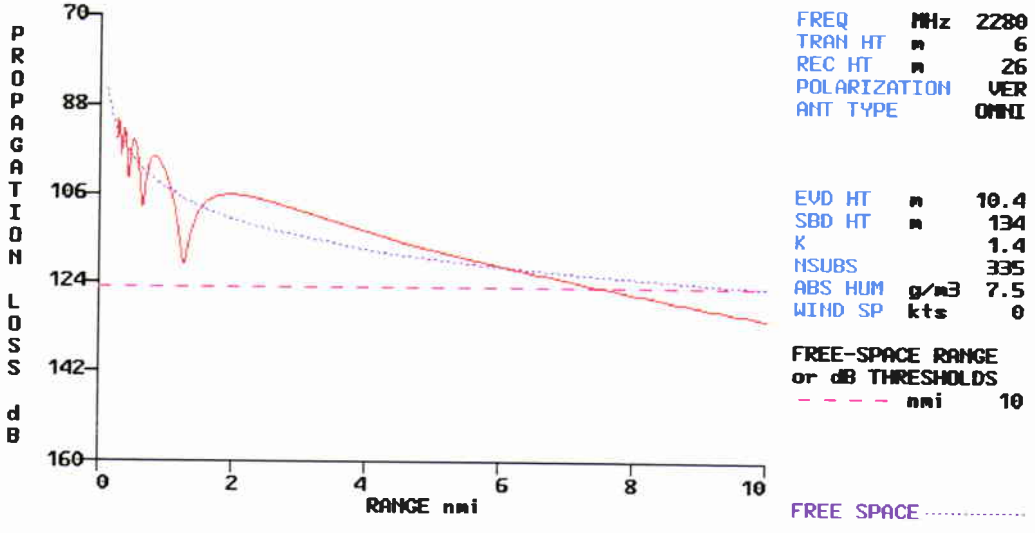

Figure B.6 *Propagation loss for test area: absence of wind, vertical polarization.*

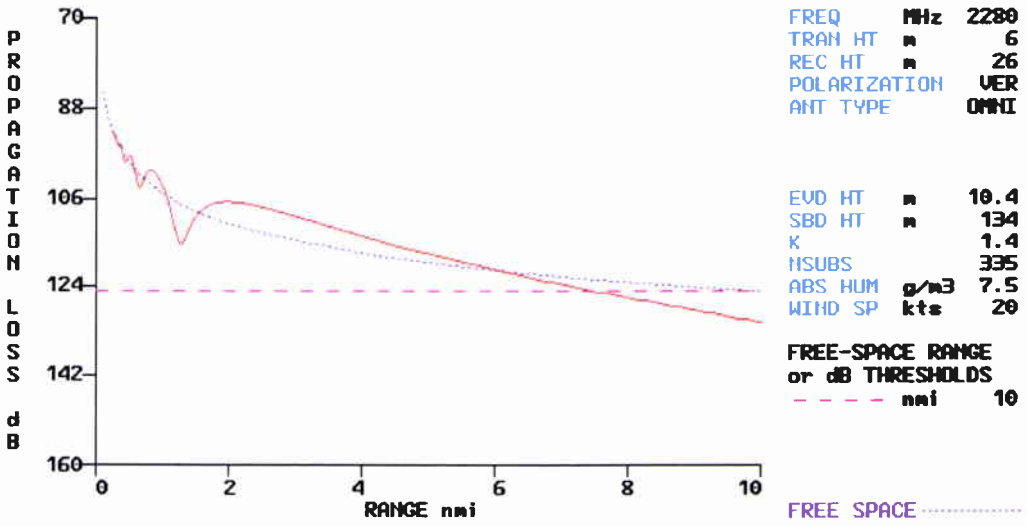

Figure B.7 *Propagation loss for test area: wind 20 kn, vertical polarization*

Annex C – Effect of Sea State on RF propagation: 400 MHz

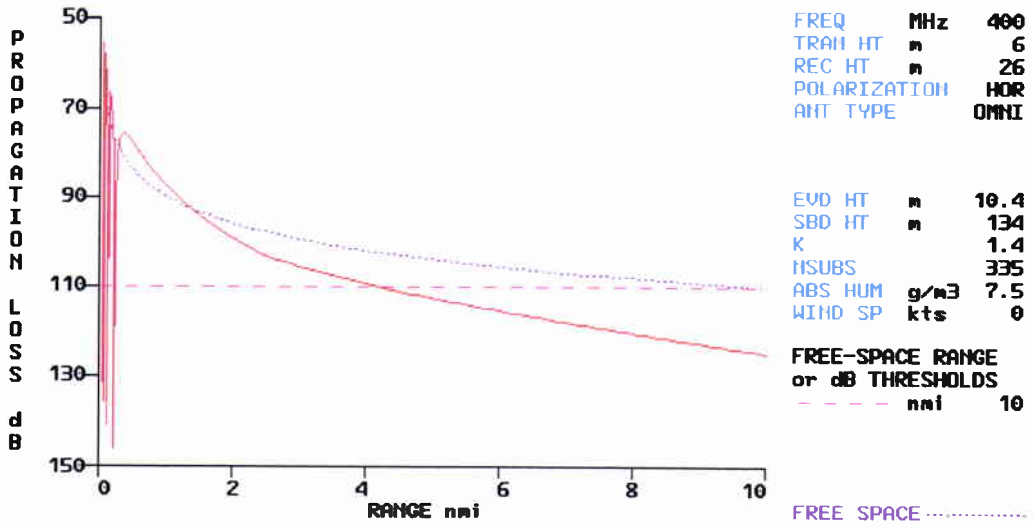

Figure C.1 *Propagation loss for test area: absence of wind, horizontal polarization*

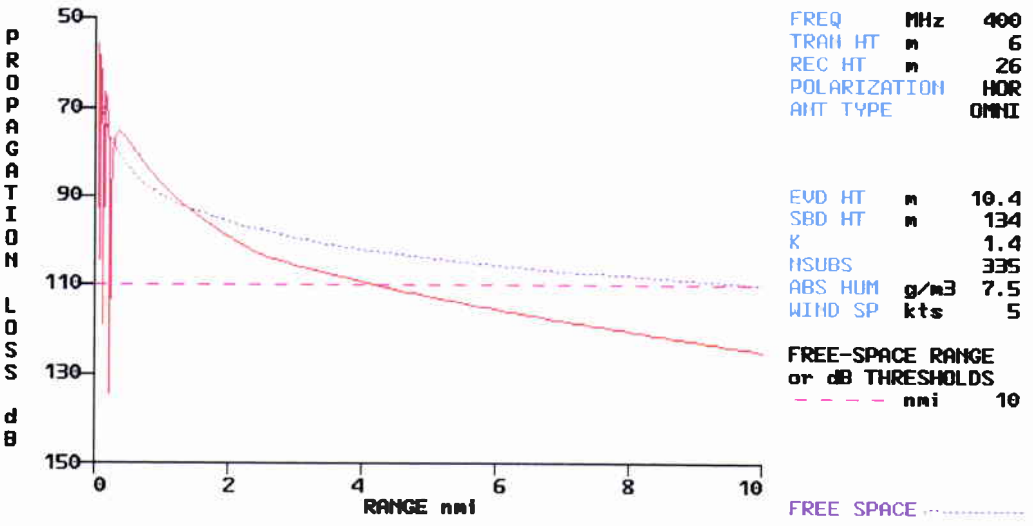

Figure C.2 *Propagation loss for test area: wind 5 kn, horizontal polarization*

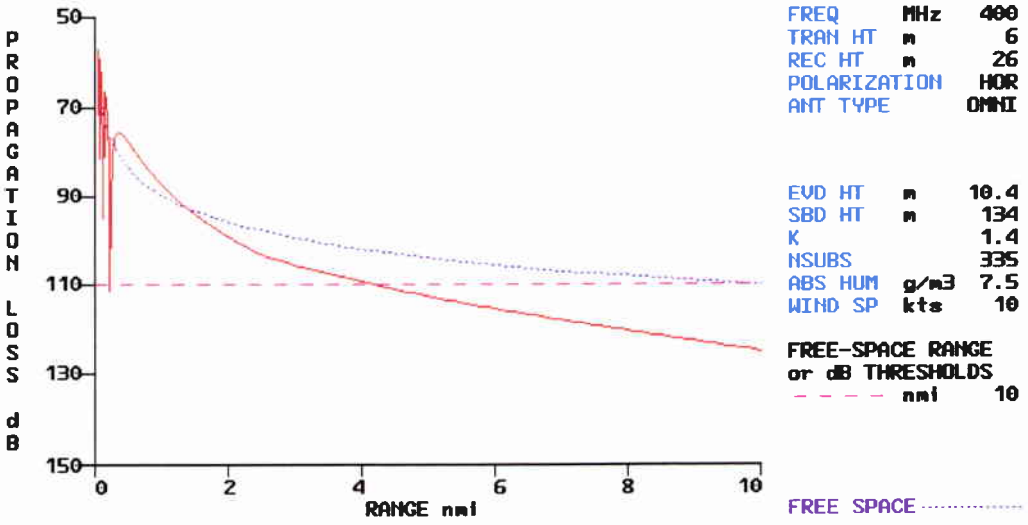

Figure C.3 *Propagation loss for test area: wind 10 kn, horizontal polarization*

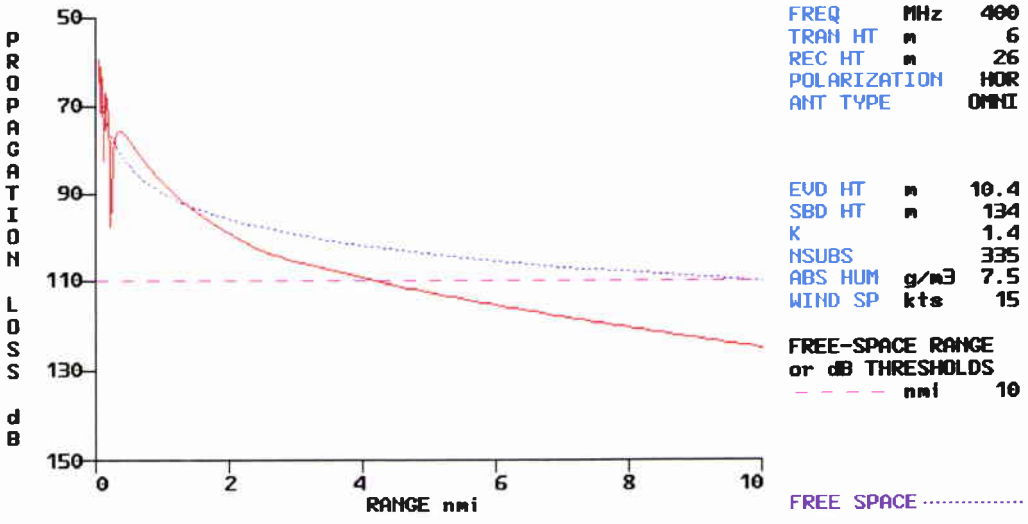

Figure C.4 *Propagation loss for test area: wind 15 kn, horizontal polarization*

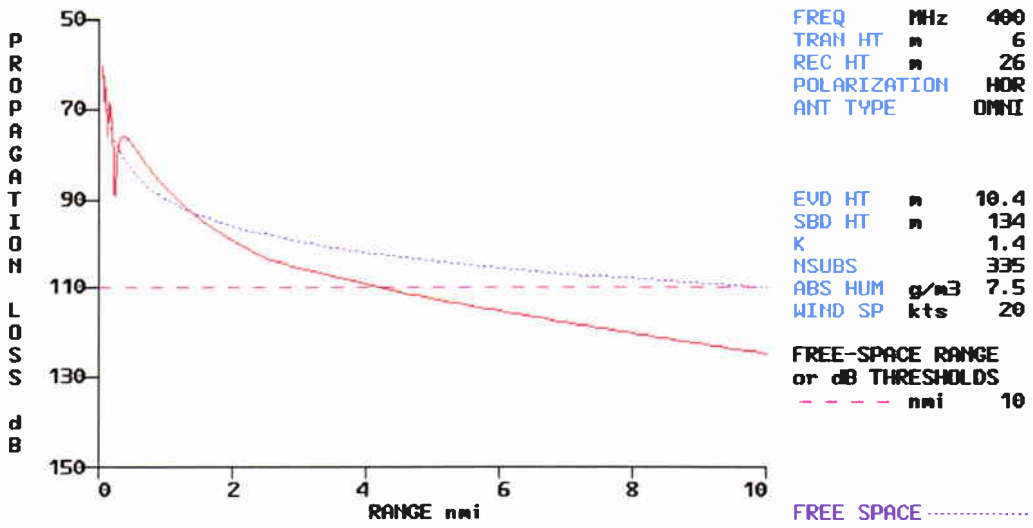

Figure C.5 *Propagation loss for test area: wind 20 kn, horizontal polarization*

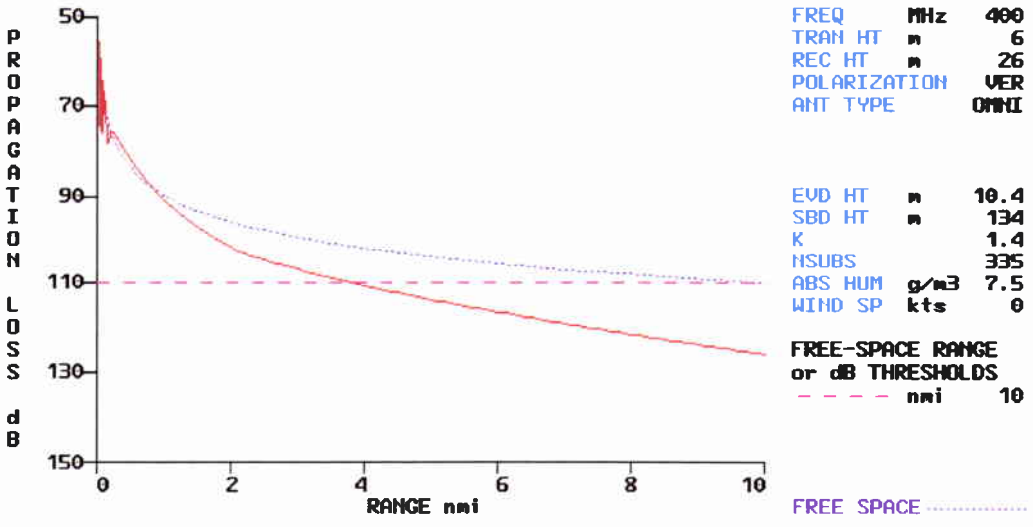

Figure C.6 *Propagation loss for test area, absence of wind, vertical polarization*

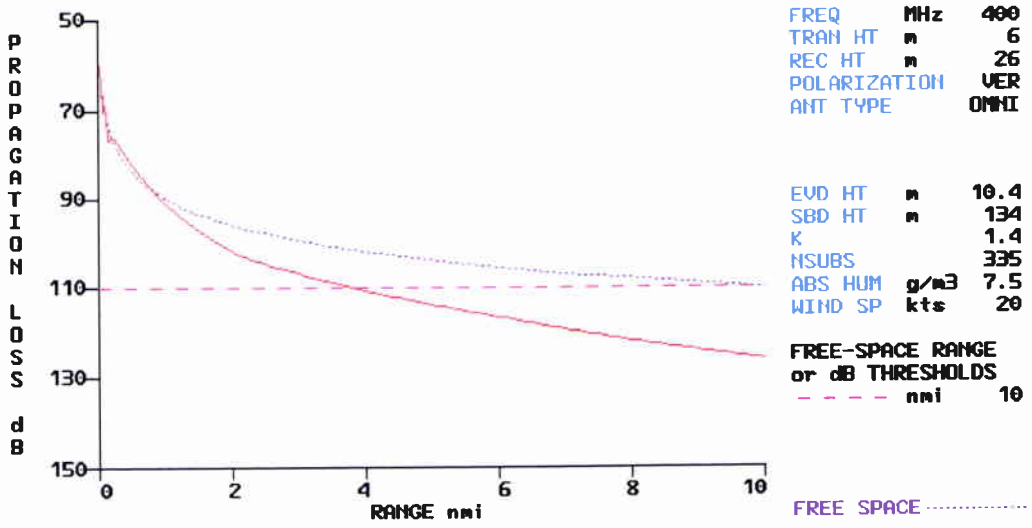

Figure C.7 *Propagation loss for test area: wind 20 kn, vertical polarization*

Annex D – Experiment of a Full Duplex Spread-Spectrum System in the 2.4 GHz frequency range

System	Cylink 128S (Direct Sequence Spread Spectrum)
Frequency	2407 – 2474 MHz
Modulation	Bi-Phase Shift Keying (BPSK), Non-Coherent Receiver
Receiver sensitivity	-92 dBm (BER 10^{-6})
Transmit power	1 – 650 mW
Channel bandwidth	10.2 MHz
Transmission delay	5.1 milliseconds
Burst period	8.5 milliseconds
Antenna type	Omnidirectional horizontal plane, 8dB gain, vertical polarization
Antenna height	33 m onboard NRV *Alliance*, 8 m onboard ITS *Ponza*

The signal quality of a spread-spectrum Cylink modem link at 2.4 GHz, 128 kbps, 0.6 Watts and the same antenna heights (7.8 – 33 m) were tested, with satisfactory results.

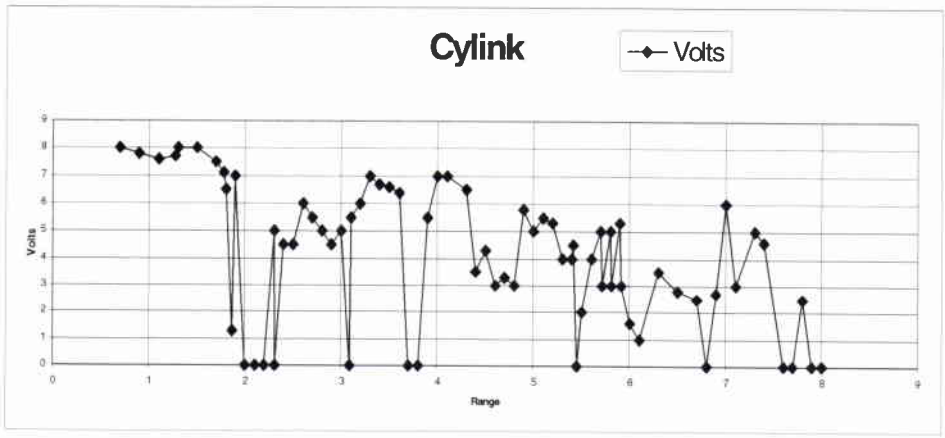

Figure D.1 *Cylink signal quality (threshold is at 4 Volts, BER = 10^{-6}) versus range during tests on 17 Nov. 98*

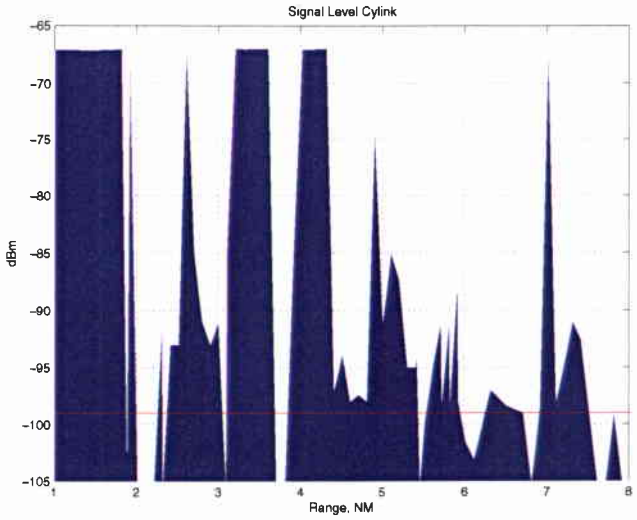

Figure D.2 *Cylink signal in dBm versus range during tests on 17 Nov. 98 The limit of signal sync loss is shown in red*

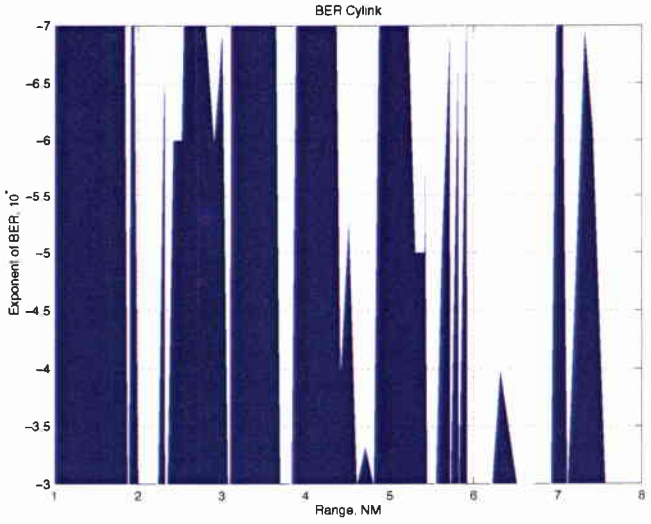

Figure D.3 *Cylink BER versus range during tests on 17 Nov. 98*

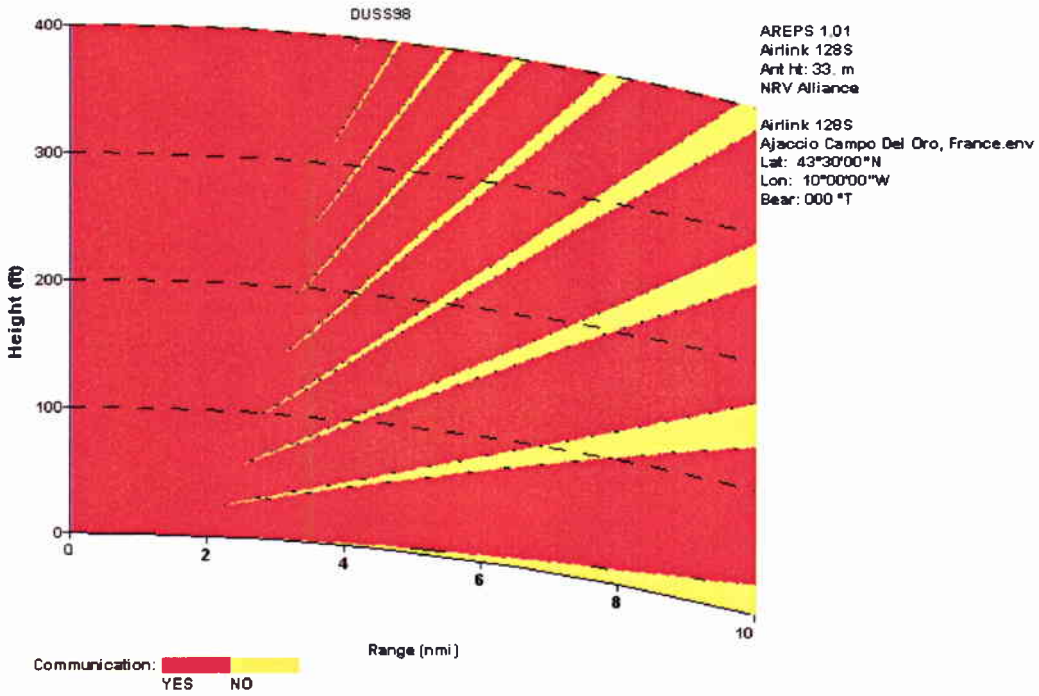

Figure D.4 *Radio coverage prediction, accounting environmental parameters*

Report no. changed (Mar 2006): SM-360 [illegible]

Document Data Sheet

Security Classification		Project No.
UNCLASSIFIED		021-1
Document Serial No.	**Date of Issue**	**Total Pages**
SM-360	October 1999	69 pp.

Author(s)

Mozzone, L., Berni, A., Guerrini, P.

Title

Long range, large throughput radio data link for DUSS (Deployable Underwater Surveillance Systems)

Abstract

Two mono-directional radio telemetry systems are described operating from a buoy to NRV *Alliance* at frequencies of 0.4 and 2.28 GHz. Digital data at 2 Mbps were transmitted close to the sea surface, collecting information on error statistics and propagation loss *versus* buoy distance, antenna height and radio parameters. A candidate system was configured for both frequency bands and the goal of 10 n.mi range was achieved. Field tests were supported by computer simulation for validation and a better insight into the results. An additional test assessed the performance of a low-power, full duplex, spread-spectrum radio link, operating at the data rate of 128 kbps, up to 3.5 n.mi. The experiments and conclusions provide useful input to the design of a Deployable Underwater Surveillance System (DUSS) for scientific and operational purposes.

Keywords

Buoy-to-buoy communication – Deployable Underwater Surveillance System – computer networks – data communication – distributed systems – radio propagation – spread spectrum communications – wireless communications

Issuing Organization

North Atlantic Treaty Organization
SACLANT Undersea Research Centre
Viale San Bartolomeo 400, 19138 La Spezia, Italy

[From N. America: SACLANTCEN (New York) APO AE 09613]

Tel: +39 0187 527 361
Fax:+39 0187 524 600

E-mail: library@saclantc.nato.int